University of Stavanger

Faculty of Science and Technology

MASTER'S THESIS

Study program/Specialization: Petroleum Engineering,	Spring semester, 2020
Writer: Ibrahem Soleman Haj Yuones	…… (Writer's signature)
Faculty supervisor: Ingebret Fjelde	
Thesis title: **Simulation of CO_2 convections in porous media**	
Credits (ECTS): 30	
Key words: Dissolution in pure water and brine. Gravitational drive. CO_2 phase diagram. CCS: carbon capture and storage. OPM- simulator. Fingers in porous media. Effect of salinity. Surface and lab cases. Diffusion coefficient. Convectional currents.	Pages: 66 Stavanger,30 /6/2020

Abstract

Global warming is one of the challenges the world faces in the modern era. Therefore, the injection of carbon dioxide into the geological layers is one of the methods which have been used to reduce the emissions of carbon dioxide.

Carbon dioxide is injected into the oil layers for enhanced oil recovery (EOR), or in the aquifers for carbon storage. When carbon dioxide is injected in water phase, water carbonate will be formed. $\mathbf{CO_2}$ dissolution initiates by the diffusion, leading to an increase in the density of water. Thus, density-driven convective flow will occur which accelerate the carbon dioxide dissolution in water.

The purpose of this master thesis has been to simulate $\mathbf{CO_2}$ convections in porous media and studying the effect of some important parameters on $\mathbf{CO_2}$ dissolution by using an open porous media flow reservoir simulator which is called (OPM). Simulation will include the impact of salinity on the dissolution of carbon dioxide by varying the concentration of NaCl in water. In addition, illustrating the effect of changing the diffusion coefficient on the dissolution of carbon dioxide and permeability as well, studying the rate of $\mathbf{CO_2}$ dissolution in porous media with absence of pure water and comparing the results with the results of real experiment which has been done at same conditions and studying the effect of permeability heterogeneity on solubility of carbon dioxide.

This master thesis is consisting of three main parts. The first part is literature study, in this part will be focused on the basic theories and fundamentals for dissolution of carbon dioxide, important physical parameters which have impact on $\mathbf{CO_2}$ dissolution and overview about carbon capture and storage (CCS). The Second part is the simulating part, here OPM-simulator will be used to illustrate and discuss the effect of changing some important parameters on $\mathbf{CO_2}$ dissolution in two different cases. The first case is **Case1**, in this case the pressure will be 100 bars and temperature will be 50 Celsius. The second case is **Case2**, in this case pressure will be 10 bars and temperature 20 Celsius (room temperature). The third part will show some limitations of using the OPM-simulator, further work as continuation of this master thesis and some personal suggestions to improve the OPM-simulator.

Further steps can be done with OPM-simulator as kind of continuation are: studying the effect of heterogeneity with more specific details like adding different horizontal and vertical

layers to see how it will affect on the dissolution of carbon dioxide. Extend the simulation to involve the dissolution of carbon dioxide in oil phase. The effect of minerals which can be founded in porous media the dissolution of carbon dioxide.

Contents

Introduction

a. Background ……11
b. Aim and objectives. ……11
c. Structure of thesis…….....11

Chapter 1

Basic theory and fundamentals for CO_2 dissolution in water.

1.1 CO_2 phase diagram. ……13
1.2 Solubility of CO_2 in water and equilibrium constants……14
1.3 Henry's law and solubility correlations……....15
1.4 Diffusion and density-driven convection mechanism in dissolution of CO_2 process**..17**

Chapter 2

(Important physical parameters on the CO_2 dissolution)

2.1 The effect of pressure and temperature on the solubility of CO_2 in water……...….18
2.2 The effect of salinity on the dissolution of carbon dioxide in brine……..19
2.3 The reaction between the carbon dioxide and the reservoir's rocks…….20
2.3.1 Reaction between carbon dioxide and carbonate rocks. …….20
2.3.2 reaction of carbon dioxide and sandstone rocks……...21
2.4 Rayleigh number…….....22
2.5 diffusion coefficient…….…..24

Chapter 3

Carbon capture and storage CCS

3.1 Introduction……..26
3.2 Carbon capturing …….....27

3.3 CO_2 transportation ……...27
3.4 CO_2 storage ……..27
3.5 Geological formations for CCS……..…..….28
3.5.1 Deep saline aquifers …….……...28
3.5.2 Depleted oil and gas reservoirs…….……...28
3.5.3 Basalt formations…….…....28
3.5.4 Unmineable coal seams…….…….…….28
3.6 Storage capacity …….…….....29
3.7 Challenges of carbon capture and storage CCS……..….31
3.8 CCS projects……..……..32
3.9 Trapping mechanisms……...…..…...33
3.10 long-term trapping analysis……..……35

Chapter 4
Simulation part (OPM-simulator)
4.1 Description of OPM……..……..37
4.2 Description of the cases ……...38
4.3 Effect of salinity on the dissolution of carbon dioxide……...40
4.4 Results of OPM-simulator VS real experiment at same conditions for both Case1 and Case2……...44
4.5 The effect of permeability on the transportation of carbn dioxide in water……..…48
4.6 Impact of diffusion coefficient on the dissolution of carbon dioxide……..50
4.7 The effect of heterogeneity on CO_2 dissolution rate……52

Chapter 5
5.1 General discussion…….……..54
5.2 Further steps can be done on OPM-simulator……..54
5.3 restrictions of OPM-simulator …….55
5.4 developing of OPM-simulator …….55

References …….……56

List of figures

Figure 1.1: Phase diagram for CO2, illustrating the different states of CO2 for different pressure and temperature conditions.

Figure (1.4.1) shows the density-driven convection during CO_2/water dissolution.

Figure (1.4.1) shows the density-driven convection during CO_2/water dissolution.

Figure (2.1): CO_2 solubility in water depends on temperature and pressure.

Figure (2.2.1) : shows Variation of CO2 solubility in water with salinity, for various conditions representative of sedimentary basins.

Figure (3.8.1) : illustrates the injection and storage of carbon dioxide on the sleipner field in north sea .

Figure (3.9.1): Examples of (a) structural and (b) stratigraphic physical traps for CO2.

Figure (3.9.2) Large-scale effect of residual trapping after injection stop.

Figure (3.10.1) Diagram showing the concept of increasing amount of immobile CO2, and thereby increased security of the storage facility.

Figure(4.3.1): simulation results of OPM-simulator showing the transportation of carbon dioxide in pure water, after 10,30,60 and 120 minutes respectively, and pressure 100 bars and temperature 50 Celsius. Permeability 76 Dacry.

Figure(4.3.2): simulation results of OPM-simulator showing the transportation of carbon dioxide in pure brine which has salinity 0.005 of NaCl, after 10,30,60 and 120 minutes respectively, and pressure 100 bars and temperature 50 Celsius and permeability 76 Darcy.

Figure(4.3.3): simulation results of OPM-simulator showing the transportation of carbon dioxide in pure brine which has salinity 0.035 of NaCl, after 10,30,60 and 120 minutes respectively, pressure 100 bars and temperature 50 Celsius and permeability 76 Darcy.

Figure(4.3.4): simulation results of OPM-simulator showing the transportation of carbon dioxide in pure brine which has salinity 0.05 of NaCl, after 10,30,60 and 120 minutes respectively, pressure 100 bars and temperature 50 Celsius and permeability 76 Darcy.

Figure(4.3.5): simulation results of OPM-simulator showing the transportation of carbon dioxide in pure brine which has salinity0.005, 0.035 and 0.05 of NaCl, after 120 minutes. Pressure 100 bars and temperature 50 Celsius and permeability 76 Darcy.

Figure (4.3.6). Simulation results of OPM-simulator showing the transportation of carbon dioxide in pure water, after 10,30,60 and 120 minutes respectively, pressure 10 bars and temperature 20 Celsius. Permeability 76 Darcy.

Figure(4.3.7): simulation results of OPM-simulator showing the transportation of carbon dioxide in pure brine which has salinity 0.035 of NaCl, after 10,30,60 and 120 minutes respectively, pressure 10 bars and temperature 20 Celsius and permeability 76 Darcy.

Figure(4.3.8): simulation results of OPM-simulator showing the transportation of carbon dioxide in pure brine which has salinity 0.05 of NaCl, after 10,30,60 and 120 minutes respectively, pressure 10 bars and temperature 20 Celsius and permeability 76 Darcy.

Figure(4.4.1). Simulation results of OPM-simulator showing the transportation of carbon dioxide in pure water, after 10,20,30,40,50,60 and 120 minutes respectively, and pressure 100 bars and temperature 50 Celsius. Permeability 76 Darcy

Figure(4.4.2). experiment results CO_2/pure water- wet porous, permeability 76 Darcy /pressure 100bars, Temperature 50 Celsius/ done by Widuramina Amarasinghe and Ingebret Fjelde, NORCE Norwegian Research Centre AS, Norway, University of Stavanger, Norway; Jan-Aage Rydland and Ying Guo, NORCE Norwegian Research Centre AS, Norway.

Figure(4.4.3): Simulation results of OPM-simulator showing the transportation of carbon dioxide in pure water, after 10,20,30,40,50,60 and 120 minutes respectively, and pressure 10 bars and temperature 20 Celsius. Permeability 76 Darcy

Figure(4.4.4). experiment results CO_2/pure water- wet porous, permeability 76 Darcy /pressure 10bares, Temperature 20 Celsius/ done by Widuramina Amarasinghe and Ingebret Fjelde, NORCE Norwegian Research Centre AS, Norway, University of

Stavanger, Norway; Jan-Aage Rydland and Ying Guo, NORCE Norwegian Research Centre AS, Norway.

Figure(4.5.1): simulation results of OPM-simulation results CO_2/pure water- wet porous, pressure 100 bars and temperature 50 Celsius. To illustrate the effect of reduction of permeability from 76 Darcy t 40 Darcy on the transportation of carbon dioxide in pure water after 2 hours.

Figure(4.5.2): simulation results of OPM-simulation results CO_2/brine (0.05 NaCl)- wet porous, pressure 100 bars and temperature 50 Celsius. To illustrate the effect of reduction of permeability from 76 Darcy t 40 Darcy on the transportation of carbon dioxide in pure water after 2 hours.

Figure(4.5.3): simulation results of OPM-simulation results CO_2/pure water- wet porous, pressure 10 bars and temperature 20 Celsius. To illustrate the effect of increasing of permeability from 76 Darcy t 760 Darcy on the transportation of carbon dioxide in pure water after 2 hours.

Figure(4.6.1). OPM-simulation results: showing the effect of increasing diffusion coefficient from $2*10^{-9}$ to $4*10^{-9}$ $\frac{m^2}{s}$ on CO_2/pure water- wet porous, permeability 76 Darcy, pressure 100 bars, temperature 50 Celsius after 2 hours.

Figure(4.6.2): OPM-simulation results: showing the effect of increasing diffusion coefficient from $2*10^{-9}$ to $4*10^{-9}$ $\frac{m^2}{s}$ on CO_2/brine (0.05 of NaCl)- wet porous, permeability 76 Darcy, pressure 100 bars, temperature 50 Celsius after 2 hours.

Figures (4.6.3): is showing the effect of reduction of diffusion coefficient on CO_2 dissolution rate in pure water-wet porous which has permeability 76 D after 115 minutes by using OPM-simulator. The diffusion coefficient reduced from $2*10^{-9}$ to $1.5*10^{-9}$ $\frac{m^2}{s}$ after 115 minutes.

Figures (4.6.4): is showing the effect of reduction of diffusion coefficient on CO_2 dissolution in brine (0.05 NaCl)-wet porous which has permeability 76 D after 115 minutes by using

OPM-simulator. The diffusion coefficient reduced from $2*10^{-9}$ to $1.5*10^{-9}\frac{m^2}{s}$ after 115 minutes.

Figure (4.7.1) is schematic drawing for the location of horizontal low permeability layer, which disturbs the homogeneity of porous media.

Figure (4.7.2) is illustrating the impact of heterogeneity on the transportation of carbon dioxide in porous media. This done at pressure 100bars and temperature 50 Celsius and time = 2 hours.

.

Figure(4.7.3) is showing the comparing of CO_2 dissolution rate between homogeneous porous media which has 76 D and heterogeneous porous media which interrupted by lower permeability layer 7.6 Darcy. This done at pressure 100bars and temperature 50 Celsius and time = 2 hours.

List of tables

Table(4.2.1) is showing the parameters which have been used at Case1
Table(4.2.2) is showing the parameters which have been used at Case2

Nomenclature

P	pressure
T	Temperature
x_{CO_2}	The molar fraction of CO2in water,
f_{CO_2}	Fugacity ofCO_2,
$K_{H.CO_2}$	Henry's constant.
R_{sb}	solubility of CO_2in brine of salinity S (scf/STB),
R_{sw}	solubility of $CO_2$of water (scf/STB),
S	salinity of brine
ρ	Density [kg/m^3].
m	Mass, units typically
V	volume, units typically [m^3]
γ	Specific weight, , has units typically [N/m^3]
g	Acceleration due to gravity, units typically [m/s^2]
K	effective permeability
Δρ	density increase of water due to CO_2 dissolution
H	the vertical thickness of diffusion
ϕ	the porosity (%)
μ	the viscosity of CO_2-rich brine
D	the CO_2 diffusion coefficient $\frac{m^2}{s}$.
V_{CO_2}	theoretical storage volume (m^3).
Vtrap	trap volume (m3)
Swirr	irreducible water saturation (%)
A	trap area (m^2)
H	average traps thickness (m).
M	reservoir capacity for CO_2storage (kg)
$\rho CO_2 r$	CO_2 density at reservoir conditions (kg/m^3)

Rf	recovery factor (%)
N	original oil in place (m^3)
Bo	oil formation volume factor
Wi	water injection (m^3)
Wp	water production (m^3)
Fig	gas injection (m^3)
G	original gas in place (m^3)
Bg	gas formation volume factor.

Abbreviations

OPM	open porous media-simulator
CCS	Carbon dioxide Capture and Storage
CO_2	Carbon dioxide
CO_3^{2-}	Carbonate ion
D	Darcy
EOR	Enhanced Oil Recovery
g	Gram
H^+	Hydrogen ion
H2CO3	Carbonic acid
HCO_3^-	Bicarbonate ion
M	Molar
mD	Millidarcy
PVT	Pressure, Volume, and Temperature
[ ]	indicates to reference number
K	Equilibrium constan

1-Introduction

a. Background

With the ever increasing population and the steady growth of industries. The demand for fossil fuels is increasing. The use of fossil fuels to obtain energy has increased carbon emissions to the atmosphere. This poses an existential challenge for humans. This led to search for ways to reduce carbon emissions.

The rapidly increase of global warming which caused by carbon emissions has led many countries and researchers to find alternative ways to reduce these emissions. Whereas, the Paris Agreement was the starting point for collective action in this field. Many developed countries have taken practical steps to reduce carbon emissions. As many large industrial countries such as China and Germany have taken effective steps such as reducing the usage of coal and replacing it with natural gas, which is less polluting the environment than coal. Also, some other countries have relied on green energy such as the hydroelectric power and solar energy to contribute to reducing global warming. The CCS project remains an important and practical step to reduce emissions of carbon dioxide in atmosphere. Norway is one of the first countries to implement this project on a large scale .Therefore, doing laboratory and program research can help a lot in developing and understanding carbon capture and storage CCS.

The dissolution of carbon dioxide has been inspected though many studies (Keith et al., 2005; [a.1]Leonenko et al., 2006[a.2]; Taku Ide et al., 2007[a.3]; Leonenko and Keith, 2008[a.4]; Hassanzadeh et al., 2009[a.5]), in which the researchers endorse that subsurface conditions are accelerating the dissolution of carbon dioxide. The effect of geometry on the dissolution of carbon dioxide studied by (Leonenko and Keith (2008)), where he used the commercial black- oil reservoir simulator. In this thesis OPM-simulator will be used to simulate the effect of some important parameters on the dissolution of carbon dioxide in porous media.

b. Aim and objectives

The aim of the present study is to show the CO_2 dissolution in porous media at different conditions and investigating the effect of some parameters like salinity, permeability, diffusion coefficient and permeability heterogeneity on CO_2 dissolution process.

This is to improve the understanding of the impact of salinity on the CO_2 dissolution process for 2 different cases (Case1 and Case2). So the objectives are:

a) Literature study to give sufficient information about CO_2 dissolution process.
b) Performing the simulation of CO_2 dissolution in different concentrations of NaCl to illustrate the impact of salinity on the total CO_2 dissolution.
c) Performing the simulation of CO_2 dissolution in porous media which contain pure water and making comparing against real experimental results. Here will be for two Cases (Case1 and Case2).
d) Performing the simulation of CO_2 dissolution for different numbers of diffusion coefficient. The aim for that is to show how the impact of diffusion coefficient on total amount of solubility of CO_2 .
e) Performing the simulation of CO_2 dissolution to illustrate the impact of permeability heterogeneity on the CO_2 transportation in porous media.

c. structure of the thesis

The thesis is organised as follows: First, a literature study is presented in 3 chapters. The first chapter shows basic theory and fundamentals for carbon dioxide for including: CO_2 phase behaviour, Solubility CO_2 of in water. Chapter 2 important physical parameters for CO_2 dissolution for instance effect of pressure, temperature and salinity on solubility of carbon dioxide in water. Chapter 3: CCS Carbon capture and storage. Chapter 4 is showing the results of OPM-simulator which will be focused on the investigation of the effects of many parameters on the dissolution of carbon dioxide. Chapter 5 will show the restrictions of using OPM-simulator, further works as extension of this master thesis and suggestions for developing of OPM-simulator.

Chapter 1

1.1 CO_2 phase diagram

The CO_2 Phase behaviour is highly dependent on temperature and pressure.

Figure 1.1 represents a phase diagram of carbon dioxide which shows 3 different phases: gas, liquid and solid phase. The point where gas, liquid and solid coexist is called the triple point. Line between the solid and liquid phase is known as the melting point line. Because it goes from a solid to a liquid because its melting and going backwards from liquid to a solid its freezing. Line between the liquid and a gas phase is called the boiling point curve. Going from a liquid to a gas its vaporization and gas to liquid is condensation. At 1 atm if you increase the temperature for carbon dioxide and we notice that it goes directly from solid to gas so carbon dioxide sublime's we can notice that at 1 atm the pressure is below the triple point. So we can say if the pressure was below of triple point it would go from a solid to gas, and if the pressure was above the triple point it would go from a liquid to a gas. But at standard pressure its bellow the triple point so that is why carbon dioxide sublime`s from solid to gas as the temperature increases. Here we can say that carbon dioxide has different densities according phase of carbon dioxide. The density of solid face of carbon dioxide is higher than liquid phase at higher pressures. Another important point is called critical point. Critical point is location where you are beyond the temperature and pressure of that point you can have supercritical fluid a supercritical fluid is a fluid that has properties of gas and liquid, it is not exactly a gas and not exactly a liquid but it is in between the two. A gas can be liquefied when the temperature is below the critical temperature.

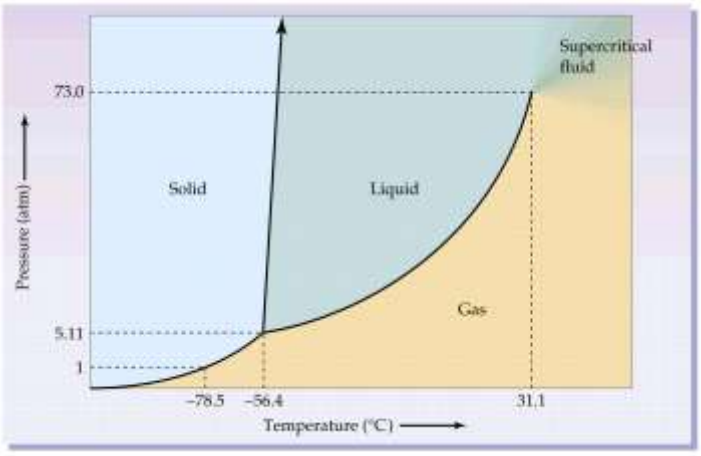

Figure1.1 Carbon dioxide (CO_2) pressure–temperature phase diagram (Whitson and Brul 2000)[1.1]

1.2: Solubility of CO_2 in water and equilibrium constants.

The amount of dissolved CO_2 is one of the critical factors to every application (experiments, modelling and simulating) Therefore, the solubility of CO_2 in water and brine must be ascertained at the condition of its application. Several CO_2 solubility studies in water and high- and low salinity brines have been conducted for an extensive range of temperatures, pressures and ionic concentration in conjunction with different reservoir properties by many researchers (Bamberger et al. 2000;[1.2.1]. Chang et al. 1998; [1.2.2]. Chapoy et al. 2004; [1.2.3]. Gui et al. 2017;[1.2.4]. Liu et al. 2011;[1.2.5].; Valtz et al. 2004;[1.2.6].). Solubility of CO_2 was investigated both in pure water an and in diverse brine solutions (Mg^{2+}, K^{+}, Na^{+}, Ca^{2+}, Cl^{-},and SO_4^{+2}) at several different temperatures and at pressures up to 200 MPa (Duan et al. 2006 ;[1.2.7]). Solubility of CO_2 and other injection gases in water and NaCl solutions is modeled at varying temperatures (0–350 C), pressures (0.1–150 MPa) and ionic concentrations (0–4.5 mol/kg) by Mao et al. (2010) [1.2.8] using Helmholtz free energy model, which can be extended to different ranges of the variables parameters.
The correlation proposed by Enick and Klara (1990)[1.2.9] on CO_2 the solubility in brine at surface condition is found to be applicable at subsurface formation conditions too, including consideration of the dissolved solids in the brine.

CO_2 dissolves in water, and some of it reacts with water molecules to produce a slightly acid solution called carbonic acid. The (aq) indicates water solution. The hydrogen carbonate compound cannot be isolated as a pure substance. It decomposes easily to produce water and CO_2 gas.

CO_2 (aq) + $H_2O \Leftrightarrow H_2CO_3$(aq) eq(1.1)

The equilibrium condition between the phases is quantified by molar solubility K_0 (henry's law) $K_0 = \frac{[H_2CO_3]}{[P_{CO2}]}$ eq (1.2)

Where is P_{CO2} is atmospheric partial pressure of carbon dioxide (in atm). K_0 is the solubility in mol L^{-1} atm^{-1} and $[H_2CO_3]$ is the dissolved CO2 concentration in mol/kg of water.This is a weak acid, so some of it dissociates to produce H^{+} ions, hence it's a slightly acidic solution, forming the hydrocarbonate ion.

$H_2CO_3 \Leftrightarrow H^+ + HCO_3^-$ eq (1.3)

$HCO_3^- \Leftrightarrow H^+ + CO_3^{2-}$ eq (1.4)

Equilibrium conditions are quantified by the acidity constants:

$K_1 = \frac{[HCO_3^-][H^+]}{[H_2CO_3]}$ eq (1.5)

$K_2 = \frac{[CO_3^{2-}][H^+]}{[HCO_3^-]}$ eq (1.6)

1.3 : Henry's law and Solubility Correlations

Henry's law is one of the gas laws states that: the amount of a given gas that dissolves in a given type and volume of liquid is directly proportional to the partial pressure of that gas in equilibrium with that liquid at a constant temperature. One of the important factors which affect the solubility of gas is Henry's constant.

Henry's constant: It is defined as the limit of carbon dioxide's fugacity(f_{co2}) to carbon dioxide water ratio (x_{co2}). K_{H,CO_2} is Henry's constant has the dimension of pressure (Eq. 1.3.1) (Diamond and Akinfev 2003) [1.3.1].

$K_{H,CO_2}(T,P) = \lim_{XCO2 \to 0} \left(\frac{f_{co2}}{x_{co2}}\right)$ eq (1.3.1)

Chang et al.(1998)[1.3.4] studied the properties of carbonated water binary system including the CO_2 solubility in water and brine to prove the eq (1.3.1) experimentally, and found that the viscosity of CO_2 - saturated water remained unchanged. For solubility measurements they used equation (1.3.2) to estimate the solubility of carbon dioxide in distilled water and later the correct it for salinity effect of brine (Kechut et al. 2011[1.3.2]) and they found agreement between the measured values and calculated values of CO_2 dissolution.

$\log\left(\frac{R_{sb}}{R_{sw}}\right) = -0.028 * S * T^{-0.12}$ eq (1.3.2)

R_{sb} solubility of carbon dioxide in brine of salinity S (scf/STB),

R_{sw} solubility of CO2 of water (scf/STB),

S: salinity of brine in weight % of solid

T: temperature (°F).

Bicarbonate (HCO_3^-), carbonate (CO_3^{2-}) and carbonic acid (H_2CO_3) are the main ions that exist when carbon dioxide is dissolving in water.

Equilibrium state established by carbonic acid (H_2CO_3) can be expressed as:

CO_2 (aq) + $H_2O \Leftrightarrow H_2CO_3$(aq) Eq (1.3.3)

To demonstrate the relation between relative carbonate ions concentration will be by mass valance equation and mass action equation:

Total Dissolved Carbon = m(H_2CO_3) + m(CO_3^{2-}) + m(HCO_3^-) Eq(1.3.4)

$\log K_1 = \log a(H_2CO_3) - \log a(H^+) - \log m(HCO_3^-)$ Eq (1.3.5)

$\log K_2 = \log a(HCO_3^-) - \log a(H^+) - \log m(CO_3^-)$ Eq (1.3.6)

$\log K_1$ and $\log K_2$ are relevant log equilibrium constants for the equilibrium.

m molality of aqueous species.

a is activity of aqueous species.

The relation between partial pressure of carbon dioxide and dissolved carbonate ions in the same solution can be expressed as:

$\log K_3 = \log p(CO_2) + \log a(H_2O) - \log a(H_2CO_3)$ Eq (1.3.7)

when the partial of carbon dioxide will increase, the dissolution of carbon dioxide will increase in the fluid. While by decreasing the partial pressure of carbon dioxide that will case to release more carbon dioxide from the fluid . as a result of CO_2 dissolution, the fluid will be more acidic. Thus, this acidic fluid will lead to dissolve more minerals from the reservoir rocks, especially carbonate minerals (perkins 2003)[1.3.3].

1.5 Diffusion and density-driven convection mechanism in dissolution of CO_2 process.

Fick's law describes the diffusion as how particles are tending to spread from a region which has higher concentration to a region of lower concentration under random thermal motion [1.4.1]. Carbon dioxide starts dissolving in aquifers by molecular diffusion (Hassanzadeh et al., 2006)[1.4.2]. The result is a thin layer in the top of the aquifers of the CO_2-saturation (Lindeberg & Wessel-Berg, 1997)[1.4.3]. when the concentration of CO_2 is increasing in water, the density of water in increasing linearly (Ennis-King & Paterson, 2005; Yang & Gu, 2006)[1.4.4]. When the thickness of water carbonate layers will increase sufficiently that will lead to gravitational instability, also in the real porous media as a result of the presence of heterogeneities in porosity and permeability will lead to appear perturbations (Emami-Meybodi et al., 2015[1.4.5]; Lindeberg & Wessel-Berg, 2011)[1.4.6]. gravitational instability and perturbations will initiate the density-driven convections (Hassanzadeh et al., 2006)[1.4.2]. as a result of density driven convection, finger of CO_2/water will migrate vertically downwards (Pau, Bell, Pruess, Almgren, Lijewski & Zhang, 2010)[1.4.7]. Unsaturated water which has less density than CO_2-saturated formation water will migrate upwards to be in contact with gas phase of CO_2. Therefore, more carbon dioxide will dissolve in water before it migrate downwards again (Pau et al. 2010)[1.4.7].

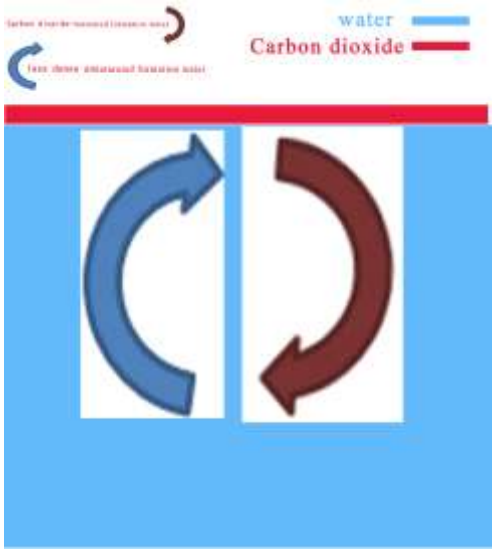

Figure (1.4.1) shows the density-driven convection during CO_2/water dissolution.

When the density-driven convection occurs, unsaturated water with respect to CO2, will migrate to the upper side of aquifer to the CO_2-water contact surface. As a result of this phenomenon the dissolution of carbon dioxide will increase. This process is significant for the projects of the carbon storage (Ennis-King & Paterson, 2005[1.4.8]; Faisal, Chevalier, Bernabe, Juanes & Sassi, 2015[1.4.9]; Kneafsey & Pruess, 2010)[1.4.10]. if the density-driven convection doesnt occur, only the upper part of aquifer will be in contact with carbon dioxide .Therefore, the dissolution of carbon dioxide in water will be governed by diffusion, which is slow process in compare to density-driven convection.

Chapter 2

Important physical parameters for CO_2 dissolution

2.1 The effect of Temperature and Pressure on solubility of CO_2 in water.

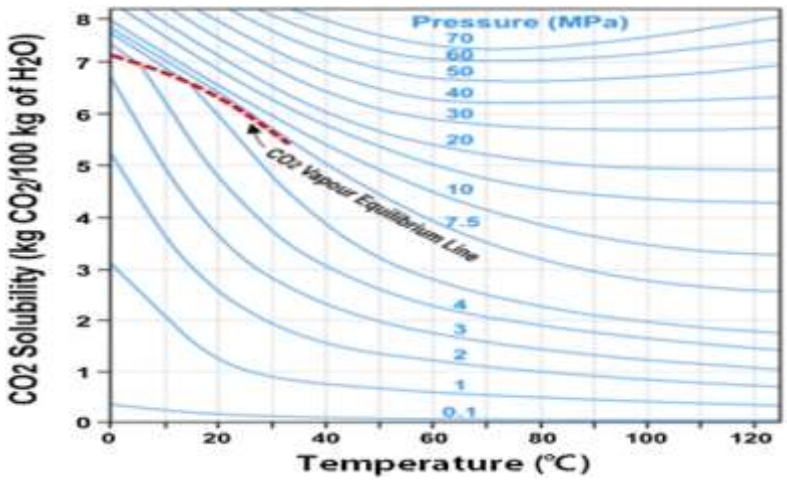

Figure (2.1) CO_2 solubility in water depends on temperature and CO_2 pressure (Perkins 2003)[2.1]

The figure (2.1) is showing the solubility of carbon dioxide in pure water as a function of temperature at different pressures. The relation between the solubility of carbon dioxide and the temperature is inverse proportionality. An increase in temperature will lead to decrease of the solubility of carbon dioxide in water Figure (2.1). There is an attractive forces between the water and carbon dioxide so when we add heat to a solution, the thermal energy will be sufficient to overcome the attractive forces which is exist between the gas and solvent molecules. Therefore, less CO_2 will be dissolved in water when the temperature is increasing. And that is why solubility in water decreases with increasing the temperature**.** Figure (2.1) shows the effect of pressure on CO_2 dissolution. The relation is direct proportion between pressure and dissolution of carbon dioxide, and the effect of pressure on CO_2 dissolution is much greater than temperature`s effect. At the constant temperature any increasing in pressure will lead directly to increase the solubility of carbon dioxide, and any drop in pressure will lead to decrease in the dissolution of carbon dioxide.

2.2 The effect of salinity on the dissolution of carbon dioxide in brine.

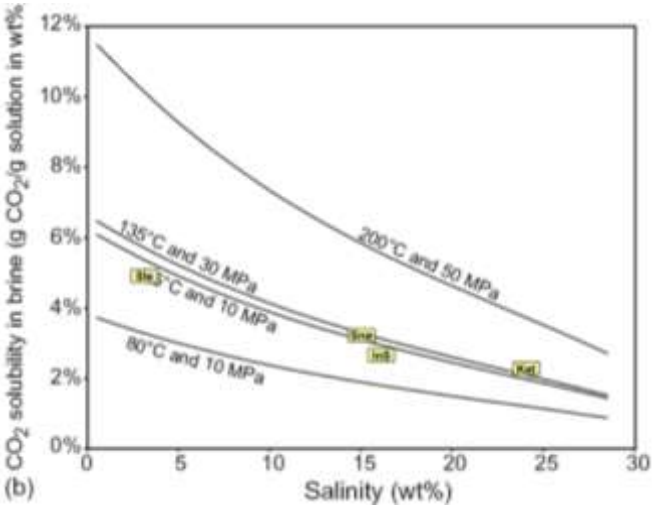

Figure (2.2.1) shows Variation of CO2 solubility in water with salinity,

for various conditions representative of sedimentary basins (Bachu & Adams, 2003).[2.2].

Salinity is one of the important factors which effects on the dissolution of carbon dioxide in water, which reduces the solubility of CO_2 gas in the water in what is known as "salting-out effect"[2.2.1] This is due to the water molecules being attracted to the salt ions, which reduces the number of H^+ and O^{2-}ions that can capture and disassociate carbon dioxide molecules. Many experiments has been done in this field, in this thesis will also the effect of salinity on the dissolution of carbon dioxide will be simulated by using OPM-simulator.

2.3 The reaction between the carbon and reservoir's rocks.

Depending on the nature and scale of the chemical reactions, CO_2 interactions with reservoir rocks and cap rocks may have significant consequences, either beneficial or deleterious, on injectivity, CO_2 storage capacity, sealing efficiency, and long-term safety and stability (Czernichowski-Lauriol et al., 1996 a,b; Rochelle et al., 2004)[2.3.1].

2.3.1 Reaction of carbon dioxide with carbonate rocks

When the rocks contain carbonate minerals such as $CaCO_3$, $MgCO_3$or $FeCO_3$, carbon dioxide can reacts with these minerals (mineral trapping) which is significant for long term of carbon capture and storage (CCS). It is known that when carbon dioxide is injected into carbonate formation, it leads to the dissolution of carbonate minerals because of the acidic nature of carbonic water. Such kind of reactions between aquifer, rocks and carbon dioxide will affect on the physical properties of the rocks. Dissolution of the rock leads to an initial increase in formation permeability; subsequently, transportation of these minerals and later precipitation lead to decrease in permeability and effective porosity (Bowker and Shuler 1991[2.3.2]; Grigg and Svec 2006[2.3.3]; Shiraki and Dunn 2000 [2.3.4]; Wellman et al. 2003 [2.3.5]).

Many factors is affecting on the this reaction such as, pressure, temperature, rock chemistry and physical conditions of the reservoir. Izgec et al. (2008) [2.3.6] observed that with the injection of carbon dioxide, porosity of core plug is changed with corresponding changes in permeability. When $CaCO_3$, $MgCO_3$or $FeCO_3$exists in the rock, the water-soluble bicarbonates might form by the following reactions:

$$H_2O + CO_2 + CaCO_3 \rightleftharpoons Ca(HCO)_2 \qquad \text{Eq (2.3.1.1)}$$

$H_2O + CO_2 + MgCO_3 \rightleftharpoons Mg(HCO)_2$ Eq (2.3.1.2)

$H_2O + CO_2 + FeCO_3 \rightleftharpoons Fe(HCO)_2$ Eq (2.3.1.3)

The rock dissolution will definitely result in the change in petro-physical properties of the rock by creating new flow paths and increasing the rock permeability.

2.3.2 Reaction of carbon dioxide with sandstone rocks.

When carbon dioxide presence in sandstone formation. There is a possibility of reduction in permeability. The explanation for that is carbon dioxide is reacting with cementing particles and releasing them and later precipitation. If the sizes of released particles are more than the pore throat size, that might abstract the pore throats, so that will lead to the reduction in permeability (Sayegh et al. 1990)[2.3.7].

The other possible reactions in sandstone formations are:

Silicates + $2H^+ \leftrightarrow M^{2+}$ + silica Eq (2.3.2.1)

$Mg^{2+}_{(aq)} + HCO^-_{3(aq)} \leftrightarrow H^+_{(aq)} + MgCO_{3(s)}$ (magnesite) Eq (2.3.2.2)

$Ca^{2+}_{(aq)} + HCO^-_{3(aq)} \leftrightarrow H^+_{(aq)} + CaCO_{3(s)}$ (calcite) Eq (2.3.2.3)

$Fe^{2+}_{(aq)} + HCO^-_{3(aq)} \leftrightarrow H^+_{(aq)} + FeCO_{3(s)}$ (siderite) Eq (2.3.2.4)

Where:

M^{2+} : generic carbon.

aq : aqueous.

S : solid.

Many experimental studies have been performed to examine the changes in the physical properties of rocks by the injection of CO_2-saturated water (Sayegh et al. 1990). Kono et al. (2014)[2.3.8] conducted experimental studies to show how the carbonated water can change

the carbonate rock properties in the reservoirs of Middle East, through core flooding at reservoir conditions, measuring porosities and permeabilities. The carbonate mineral dissolution studies were conducted on scanning electron microscope (SEM) and liquid chromatography also. Results obtained (without the compaction effects) showed an increase in porosity by a 3.6% in the first 50 pore volume injected, and a further increase in up to 6.0% from 50 to 100 pore volume injected.

2.4 Rayleigh number

Rayleigh number (Ra) is a dimensionless, measures as a ratio of free convection to diffusion [2.4.1],[2.4.2]. The Rayleigh number provides an indication of whether density-driven convection will take place under given properties and conditions (Kneafsey & Pruess, 2010). Low Rayleigh numbers correspond to pure molecular diffusion because perturbations within the system are observed to decay. When the Rayleigh number exceeds a critical value, Ra_c = $4\pi^2$ observed that the perturbations are growing, and density-driven convection will occur Hassanzadeh et al., 2006; Kneafsey & Pruess, 2011; Khosrokhavar et al., 2014[2.4.3]; Lindeberg & Wessel-Berg, 1997; Xu et al., 2006). Furthermore, when the Rayleigh number is increasing the density-driven will increase (Farajzadeh, Ranganathan, Zitha & Bruining, 2011)[2.4.4].

Rayleigh number is functional with properties of fluid and porous media. The Rayleigh number can be written as:

$$Ra = \frac{K\Delta\rho g H}{\varphi \mu D} \qquad \text{Eq (2.4.1)}$$

K is the effective permeability (m^2)

$\Delta\rho$ density increase of water due to dissolution of carbon dioxide ($\frac{Kg}{m^3}$)

g is the gravitational acceleration ($\frac{m}{s^2}$)

H is the vertical thickness of porous media

φ is the porosity. (-)

μ is the dynamic viscosity. (Pa.s)

D is diffusion coefficient of carbon dioxide in water. ($\frac{m^2}{s}$)

The effective permeability according to the Hele-Shaw cell with uniform thickness, the porosity is 1.

$K = \frac{b^2}{12}$ Eq(2.4.2) [2.4.5][2.4.6]

Where is the b is the uniform thickness of Hele-Shaw cell.

The gravitational instabilities can be occurred only when the diffusive layer is thick enough that Rayleigh number will be more that critical value Ra_c [2.4.7]. Nield [2.4.8]offered method to measure the critical Rayleigh number which is 32.5 as estimated by Slim and Ramakrishanan [2.4.9] based on linear stability analysis, 55 as estimated by Szulczewski et al[2.4.10], and 31.5 as estimated by Slim [2.4.11] according to the theoretical analysis of dissolution rate.

A critical onset time (t_c) and critical wavelength (λ_c) were widely used to predict the gravitational instabilities.

The critical onset time (t_c) can be predicted as[2.4.17]

$t_c = a_1 D(\frac{\varphi\mu}{K\Delta\rho g})^2 \approx a_2 Ra^{-2}$ Eq (2.4.3)

Where a_1 and a_2 are the parameters for the onset time of convection.

The critical wave length λ_c can be calculated as [2.4.12][2.4.19][2.4.13]

$\lambda_c = \frac{a_3 \varphi\mu D}{K\Delta\rho g}$ Eq (2.4.4)

Density-driven convection enhances the CO_2dissolution rate with the increase in Rayleigh number. Islam et al[2.4.14]. indicated that effective convection occurred only at a limited range of scales when Rayleigh numbers exceeded the critical value.

2.5 diffusion coefficient D

Diffusion coefficient is one of critical factors which has impact on density-driven convection of dissolution of carbon dioxide in water. Diffusion coefficient also known as the diffusivity, describes how fast one material can diffuse through another material. The higher diffusion coefficient, the faster diffusion will be. Therefore, the diffusion coefficients for solids tends to be much lower than the diffusion coefficients for liquids and gases.

The **Arrhenius** formula to calculate the diffusion coefficient as follow:

$D = D_0 \cdot e^{\frac{-E_A}{RT}}$ Eq (2.5.1) [2.5.1][2.5.2]

D: diffusion coefficient ($\frac{cm^2}{s}$).

D_0 : pre-exponential factor.

E_A : activation energy ($\frac{J}{mol}$).

R : gas constant (8.314 $\frac{J}{mol.K}$)

T: temperature (K)

To study how the diffusion coefficient is affecting of the density-driven convection, that can be by Rayleigh number eq (2.4.1). In eq (2.4.1) the diffusion coefficient D is dominator in the equation, so the relation between Ra and D is inverse proportion. By increasing the diffusion coefficient the Rayleigh will decrease, that means less density-driven convection will occur. When diffusion coefficient is decreasing, the Rayleigh number will increase. Thus density-

driven convection will accelerate. PVT cell experiments were also performed by Farajzadeh et al. (2007)[2.5.3]at a pressure 50 bars and temperature of 30 ˚C. At early stages, the effective diffusion coefficient was found to be one order of magnitude larger than for pure molecular diffusion of CO_2into water.

Chapter 3

Carbon capture and storage (CCS)

3.1 introduction

Climate change is one of the major challenges of our time. The greenhouse gases emissions have continuously increased since the industrial revolution (Stocker et al., 2013)[3.1.0], leading to global warming.
Over the past decades, the atmosphere and ocean temperature have risen, the amount of snow and ice have diminished and sea level has increased as results of the global warming. International agreements (EuropeanCommission, 2012, 2010; Kioto Protocol, 1997; Paris Agreement, 2015; Rio Summit,1992) highlight the necessity to take climate protection actions.
The increase of renewable energy generation, the implementation of carbon capture and storage (CCS) and the improvement of energy efficiency are the most promising options to reduce greenhouse gases emissions (Edenhofer et al., 2014)[3.1.1].

Carbon capture and storage (CCS) divided of three main steps:

1- Capturing waste carbon dioxide from large point sources (i.e. fossil fuel power plants, cement industries...).
2- Transporting carbon dioxide to site that will be injected.
3- Storing it into underground geological formations (Metz et al., 2005)[3.1.2]. The CO_2 should be confined in the subsurface for a long time period preventing the release of carbon dioxide to the atmosphere again.

3.2 carbon capturing

The first and most difficult step in CCS is to remove the carbon dioxide from other gaseous substances because the smoke from power plants is not only contains carbon dioxide but also other substances. Carbon capture is considered as an expensive process so will not be easy to implement it in all over the world.

Many methods can be used to capture the carbon dioxide for instance,

a- post-combustion separation:

here they separate the carbon dioxide from flue gas emitted from power plants by using adsorption of the gas in the solvent for instance: using the chilled ammonia process which we use ammonia as a solvent [3.2.1].

b- Oxyfuel separation

it considers as advanced way to capture carbon dioxide. When the fuel is burnt in air the carbon dioxide will react with other components of air for instance nitrogen[3.2.2].

c- pre-combustion separation

which means gasification of fuel like natural gas or coal and convert it to carbon monoxide and hydrogen (syngas) mixture.

3.3 CO_2 transportation

After capturing the carbon dioxide, it must be transported to the storage site. But first they liquefied the carbon dioxide then they decide to which method for transport will be used.
If we have small-scale they transportation will be by boats, trucks and rail-ways.
But when we have large-scale usually pipeline will be used.

3.4 CO_2 storage

This last step in CCS, when carbon dioxide will be transported to storage site it needs to be stored. Selecting the storage site is depending on the potential of this site and cost-effectiveness. Carbon dioxide can be stored in geological formations of oceans. Storage in oceans is considered as a high environmental risk therefore no longer has been used.
Nowadays they store carbon dioxide just in geological formations. [3.3.1]

3.5 geological formations for CCS

Many geological formations can be used as storage sites.

3.5.1 Deep saline aquifers

This refers to water reservoirs. They are considered to be one of the best choice for the storage of carbon dioxide due to their geographical ubiquity and large potential of storage.[5.1.1]

3.5.2 Depleted oil and gas reserves

Here carbon dioxide is injected into such depleted hydrocarbons reservoirs. This method known as enhanced oil recovery (EOR). But this method will be considered as high price scenario if the reservoirs will not be extensive.

The incremental oil production can reach to 180 million barrels and around 60 million tons of carbo dioxide can be stored annually with help of $CO_2 - EOR$.[3.5.2]

3.5.3 Basalt formations.

This volcanic rock has silicates of metals such as calcium, iron and aluminium which can react with carbon dioxide and form the carbonate minerals which considers as very good site to store the carbon dioxide.[3.5.3]

Advantages of such sites are:

a- the trap will be considered as stable.

b- High level of security for the storage because the reaction between carbon dioxide and silicates of metals will give mineral carbonate which is suitable for long term of storage.

c- high level of integrity for carbon dioxide storage because basalt provides solid cap rocks.

3.5.4 unmineable coal seams

At deeper depths such recovery is not economically feasible. Thus, the captured CO2 can be injected in such seams, which improves methane recovery. This is known as enhanced coalbed methane recovery (CO2–ECBM). It is seen that the injection of CO2 not only improves methane extraction, but also helps to make the adsorption of carbon dioxide much more rapid.[3.5.4]

3.6 storage capacity

According to Bradshaw et al. [3.6.1], capacity can be threefold according to the required category level:

a. theoretical, realistic and viable capacity.

Theoretical capacity is considering that the entire porous is available for storage or they consider that aquifers have maximum dissolution of carbon dioxide. but practically will be impossible to reach the theoretical level.

b. realistic capacity: takes in the consideration the real parameters of reservoir (permeability, porosity, depth etc.).

c. viable capacity: includes the consideration of legal limitations and considerations of social and environmental aspects of the selected site for storage.

Storage capacity can be defined as the quantity of carbon dioxide that maybe Injected and stored in the geological layers.

According to the study of the Task Force for Review and Identification of Standards for CO2 Storage Capacity Estimation of Carbon Sequestration Leadership
Forum (CSLF), the regional CO2 storage capacity in structural and stratigraphic traps can be calculated using a residual water saturation [3.6.2], [3.6.3]:

$$V_{CO2t} = V_{trap}.\Phi.(1 - S_{wirr}) = A.h.\Phi(1 - S_{wirr}) \qquad \text{Eq (3.6.1)}$$

V_{CO2t} : Theoretical storage volume of carbon dioxide (m^3)

V_{trap} : Trap volume (m^3)

Φ : Porosity (%)

S_{wirr} : Irreducible water saturation (%)

A: Trap area (m^2)

h: Average trap thickness (m)

According to the United State Department of Energy (US DOE), for the regional salt water aquifers, the coefficient of storage efficiency is suggested to be 2% [3.6.4]. [3.6.5]

The storage capacity of depleted hydrocarbon fields can be calculated from cumulative production and reserve data following the methodology described in [3.6.6]

$M = \rho.CO_{2r}(R_f.N.B_{fo}\text{-}W_i - W_P)$ Eq (3.6.2)

$M = \rho.CO_{2r}.R_f\,(1\text{-}F_{ig}).G.B_g$ Eq (3.6.3)

M: capacity of reservoir for carbon dioxide storage (kg)

$\rho.CO_{2r}$: density of carbon dioxide at reservoir conditions (kg/m^3) .

R_f : recovery factor (%).

N: original oil in place(m^3).

B_g : gas formation volume (%).

B_o : oil formation volume (%).

W_i : water injection (m^3).

W_P : water production (m^3).

F_{ig} : gas injection (m^3).

G : gas original in place (m^3).

For the effective capacity it is necessary to consider some additional factors such as the macroscopic displacement efficiency, buoyancy, reservoir heterogeneity, water saturation, reservoir drive, etc.

The first global assessment of carbon dioxide storage capacity back to the 1990s. Koide et al. [3.6.7], [3.6.8] assessed carbon dioxide storage capacity for deep saline aquifers on the level of $320*10^9$ tons. According to Van der Meer [3.6.9], it was estimated to $425*10^9$ tons, calculation made by Ormerod et al. [3.6.10] was on the level of 790 $*10^9$ tons of carbon dioxide. Hendricks and Blok [3.6.11] reported storage capacity of $150*10^9$tons, which was mainly related to depleted hydrocarbon reservoirs [3.6.12].

3.7 challenges of carbon capture and storage (CCS)

a. Geological storage complex and surrounding area characterisation:

Potential sites for geologic storage are: depleted oil and gas fields, deep saline formations and deep unmineable coal seams. According to EU Directive 2009/31/EC [3.7.1], the characterisation and assessment of the potential storage complex, including the cap rock and surrounding area, including the hydraulically connected areas, should be carried out in three steps according to best practices at the time of the assessment: (1) data collection, (2) building the three-dimensional static geological earth model and (3) characterisation of the storage dynamic behaviour, sensitivity characterisation and risk assessment.

b. Potential of CO_2 leakage pathways:

The possibility of potential leaks of carbon dioxide is one of the hardest barriers to large-scale of carbon capture and storage.

The injected CO_2 can migarte from the storage formations upwords (into atmosphere, aquifers or upper formations) if these following conditions will exist: 1. When the gas pressure will be higher than capillary pressure. 2. When there is gap in cap rocks that will lead carbon dioxide to migrate to upper aquifers. 3. Fault in siltstone that will force carbon dioxide to migrate to upper aquifers. 4. CO_2 will esacpe to atmosphere via poorly sealed new or abandoned wells.

Possibility of leakage of carbon dioxide from the active or an abandoned well include leakage: corrosion of the tubing, around packer, through deterioration of the casing, between the outside of the casing and the set cement, through the deterioration of the set cement in the annulus.

leakage in the annular region between the set cement and the formation, through the cement plug and between the set cement and the inside of the casing [3.7.2]. [3.7.3]. [3.7.4].

3.8 CCS projects

Carbon capture and storage is considering as new technology, therefore the implementation of this project will have many obstacles which can preventing the moving from planning stage to construction stage and operation phase.

Several years of worldwide implementation of carbon capture and storage programs have resulted to sufficient data and knowledge on CCS technology. Comprehensive databases founded by, for example, Carbon Capture and Sequestration Technologies at the Massachusetts Institute of Technology (MIT) [3.8.1], Global CCS Institute [3.8.2], National Energy Technology Laboratory (NETL) [3.8.3 18], Zero Emissions Platform [3.8.4], British Geological Survey [3.8.5], etc., can serve as a valuable source of information in further research and design [3.8.6]. A large-scale facility captures at least 0.8 Mt of CO2 from a coal-based facility for power generation or at least 0.4 Mt of CO2 from other industry on yearly basis [3.8.2].

The Global Carbon Capture and Storage Institute database counts 23 large-scale CCS facilities both in operation and under construction, having capture capacity of approximately 30 Mt/y. Realisation of further 5 projects, which are now in advanced planning phase, as well as another 15 projects, which are in early planning, could significantly increase capture capacity by more than 60 Mt/y. Temporarily ongoing large-scale CCS projects are located in the USA, Canada, China, Saudi Arabia, United Arab Emirates and Europe. The most promising CCS projects. However, successful operation of two Norwegian large-scale projects (Sleipner and Snøhvit).

According to the Norwegian ministry of petroleum and energy:

- During processing of natural gas from the Sleipner Vest field nearly one million tonnes of carbon dioxide per year has been separated, and stored in the Utsira formation.
- Natural gas production at utgrad field has been separated the carbon dioxide at the sleipner platform and stored in the Utsira formation(since 2019).
- Snøvit facility is separating carbon dioxide from the well stream and captured carbon dioxide is back to the Snøhvit , around 700000 tonnes every year of carbon dioxide is stored there.

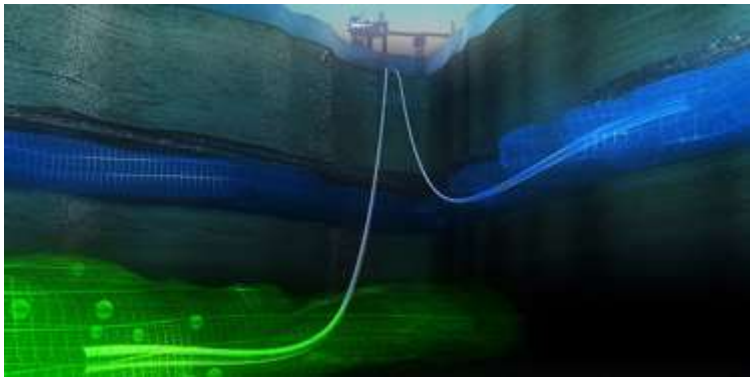

Figure (3.8.1) illustrates the injection and storage of carbon dioxide on the sleipner field in north sea (photo: alligator film/BUG, Equinor)

3.9 trapping mechanisms

Four different storage mechanisms keep the supercritical CO2 securely stored inside the CO2 storage formation:

(1)structural/stratigraphic (or physical) trapping.

(2) solubility trapping.

(3) residual trapping.

(4) mineral trapping [3.9.1]. [3.9.2].

1. structural/stratigraphic (or physical) trapping.

   Physical trapping of carbon dioxide will be below the cap rocks which are low permeability seals, for instance shale or salt beds.

   Physical trapping simply means to store carbon dioxide in geological formations. Sedimentary basins can be considered as physical trap. The lateral change in rocks caused by variation in the setting where the rocks deposited can make stratigraphic traps.

   In saline formations that don't have much distance that can be considered as structural trapping. When carbon dioxide is injected into structural trapping it displaces saline formation water and then migrates buoyantly upwards, because it

is less dense than the water. When it reaches the top of the storage formation, it continues to migrate as a separate phase until it is dissolved (potentially helped by gravity instability and mixing), trapped as residual CO2 saturation or gets arrested in local structural or stratigraphic traps below the sealing formation (IPCC 2005)

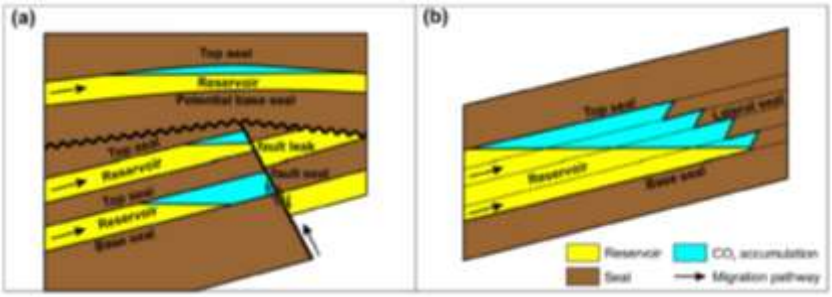

Figure (3.9.1): Examples of (a) structural and (b) stratigraphic physical traps for CO2 (From CO2CRC, 2008).

2. **Solubility trapping**

Dissolving the carbon dioxide in water formation is known as solubility trapping. The advantage of this trapping that when carbon dioxide is dissolving in water, it no longer exists as a separate phase. As underlined by various authors (Bachu et al. 2007), CO2 dissolution is a significant trapping mechanism and saturating formation water with carbon dioxide would create huge carbon dioxide storage capacities (Bachu & Adams, 2003). Nevertheless, it is also indicated that dissolving carbon dioxide is a long-term process, coupling molecular diffusion and in some cases aided by gravitational instabilities in the formation water.

3. Residual trapping

When supercritical carbon dioxide injected in porous rocks which are water saturated, small droplets of supercritical carbon dioxide will be trapped and left behind due to the variation of the capillary properties of the pores. This called residual trapping. This kind of CO_2 trapping is very secure for CO_2 storage because residual trapping is immobile.

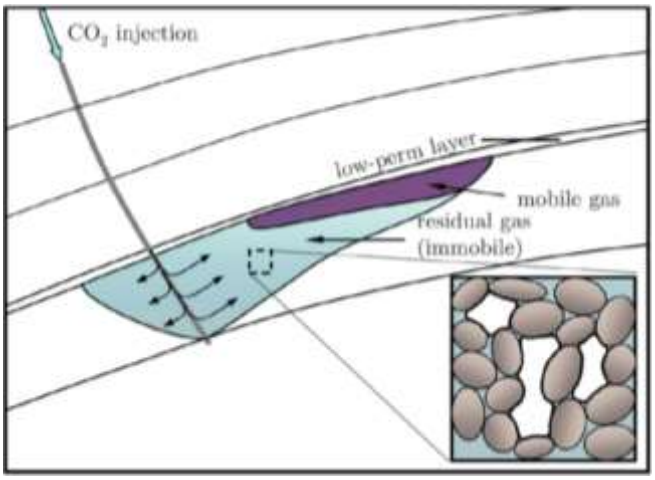

Figure (3.9.2) Large-scale effect of residual trapping after injection stop (Juanes et al. 2006)

4. Mineral trapping

   Due to the increment the acidity of water as a result of dissolution of super critical carbon dioxide, and it subsequently induces the dissolution of primary mineral compositions in liquid phase. Dissolving the carbon dioxide can react with minerals in a geologic formations, that will cause the sedimentation of secondary carbonate minerals for instance calcite $CaCO_3$, dolomite $CaMg(CO_3)_2$, siderite $FeCO_3$ by a servals of reactions with aqueous ions in the saline aquifers. This processes is called mineral trapping (Bachu et al., 1994) Mineral trapping is considered as the most promising long term for carbon capture and storage.

3.10 Long-term trapping analysis.

Most of the injected carbon dioxide will be mobile (Kneafsey & Pruess, 2010)[3.10.1]. Thus, physical trapping dominates in the early stages. The figure (3.10.1) (IPCC report 2005. Chapter 5) is illustration of the different trapping mechanism and storage(the change in storage of carbon dioxide by the time). At early time the physical trapping will dominate, over time the security of storage can increase when we have more residual and solubility trapping. But most secure and promising for long term storage is mineral trapping (Kneafsey & Pruess, 2011).

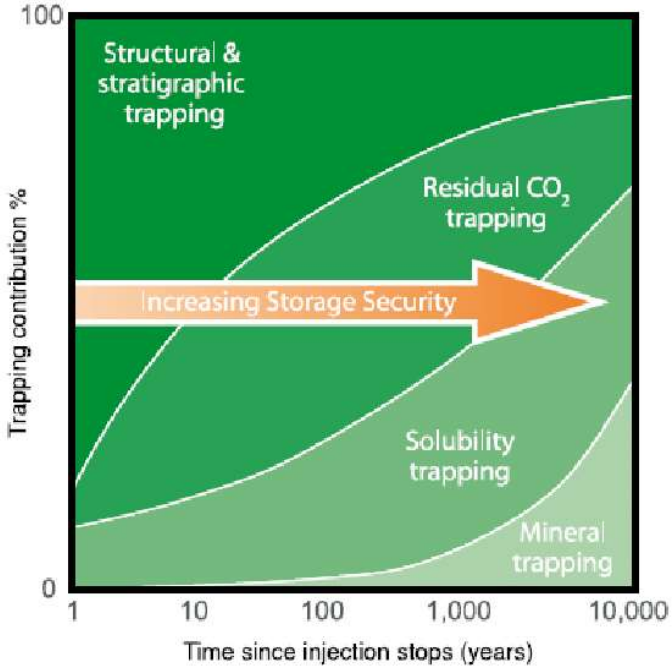

Figure (3.10.1) Diagram showing the concept of increasing amount of immobile CO2, and thereby increased security of the storage facility. The mechanisms responsible for the immobilisation of CO2 are shown. From IPCC 2005. Right) Trapping-mechanism/time diagram based on data from simulations of the processes of mineral reaction and dissolution. Produced from data given for a base-case study (Zhang et al. 2009). (Figure from Frykman et al. 2010).

Chapter 4:

OPM- SIMULATOR

4.1 description of OPM

The open porous media (OPM) is a collaborative effort, which encourages more researches for simulation of porous media processes. Open Porous Media software components have been developed by:

Research institutes (NORCE, SINTEF,)

Companies (Equinor)

Universities (U. Stuttgart, university of Bergen and NTNU)

The purpose of initial version was for open-source software for simulating the transport and flow in porous media. Then it extended to supply open data sets, so in this way will make it easier to test different models, benchmark and computational methods. Reservoir simulation is the main field that OPM is focusing about. Therefore OPM is focusing about the tools which are related with reservoir simulation.

OPM software contains

OPM flow : it is a reservoir simulator using fully-implicit discretization and using automatic differentiation [4.1.0] to avoid the error in derivation and coding of Jacobians for residual equations. OPM flow in turn builds or uses on frameworks and libraries such as dune [4.1.1], DuMuX [4.1.2], Zoltan [4.1.3], and Boost to reduce implementation and maintenance cost and improve software quality. The Matlab Reservoir Simulation Toolbox [4.1.4], [4.1.5], [4.1.6],has also been source of ideas and concepts.

Upscaling tools: it is using steady-state approach and contains programs which can do upscaling of capillary curves, flow-based permeability and relative permeability.

Para View : an easy tool and uses for quick visualization of the reservoir simulation.

In this thesis (simulating of Co_2) convections we did as follow :

A. Input : tables which contains the codes

1- Tables for CO_2 fluid properties calculated [4.1.A]

2- Co_2-solubility in brine and water solubility in the Co_2-phase are implemented after Duan & Sun, [4.1.A2]

B. Building and running the problem(CO_2injection − uncover) on Linux which Ubuntu has been used.
C. Visualization: ParaView used as monitor for the results

4-2 : description of Cases

In this part of the master's thesis, simulation results will be presented and discussed in two different cases: Case 1 (labcase), in this case the simulation will be done at a pressure of 100 bars and a temperature of 50 degrees Celsius. These values were chosen to compare the simulation results with the experimental results that performed under the same conditions [4.2.1]. Case 2 (surface case(as a name)), in this case the simulation will be done at a pressure 10 bars and a temperature 20 degrees Celsius ; furthermore, the results of simulation will be compared with experimental results [4.2.2].
Table (4.2.1) shows the parameters which has been used to simulate Case1. Table (4.2.2) shows the parameters which has been used to simulate Case 2. In both Case 1 and Case 2 are homogeneous porous media but we add some noise in OPM-simulator to generate fingers when the carbon dioxide dissolves in water. Boundary conditions in Case1 and Case2: Top boundary: Free-flow boundary condition. Left, right and bottom boundaries: no-flow boundary condition. Porous media will be saturated with either pure water or with brine which has different concentrations of NaCl.

Case1 lab case		
Parameter	Numerical value	Unit
Pressure	100	Bars
Temperature	50 Celsius	Celsius
Permeability	76	Darcy
Permeability of left, right and bottom boundaries (almost impermeable)	$76* 10^{-9}$	Darcy
Diffusion coefficient	$2*10^{-9}$	$\frac{m^2}{s}$

Table (4.2.1): parameters of Case1

Case2 (surface case)		
Parameter	Numerical value	Unit
Pressure	10	Bars
Temperature	20 Celsius	Celsius
Permeability	76	Darcy
Permeability of left, right and bottom boundaries (almost impermeable)	$76* 10^{-9}$	Darcy
Diffusion coefficient	$2*10^{-9}$	$\frac{m^2}{s}$

Table (4.2.2): parameters of Case2

4-3: Effect of salinity on the dissolution of carbon dioxide in brines.

The effect of salinity on the solubility of carbon dioxide in water will be examined by OPM-simulator at Case1 and Case2.

First for Case1, figure (4.3.1) shows the simulation results when the porous media has pure water. Figure (4.3.2) shows the simulation results when porous media has brine with low concentration of NaCl (0.005). Figure (4.3.3) illustrates the simulation results when the water contains 0.035 of NaCl. Figure (4.3.4) shows the simulation results when the salinity in increased to 0.05 of NaCl. All figures have done at same time steps 10, 30, 60 and 120 minutes respectively.

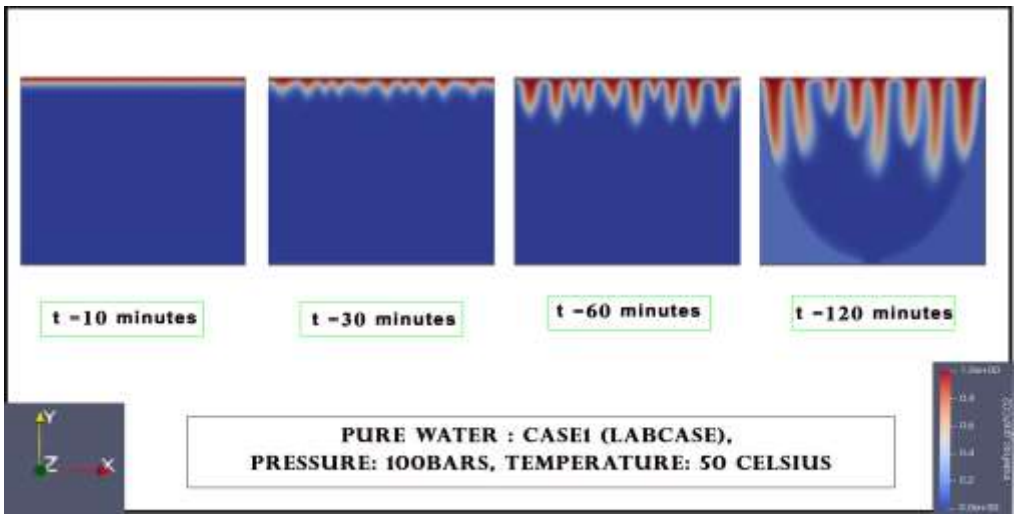

Figure(4.3.1). OPM-simulation result CO_2/pure water-wet porous, permeability 76 Darcy

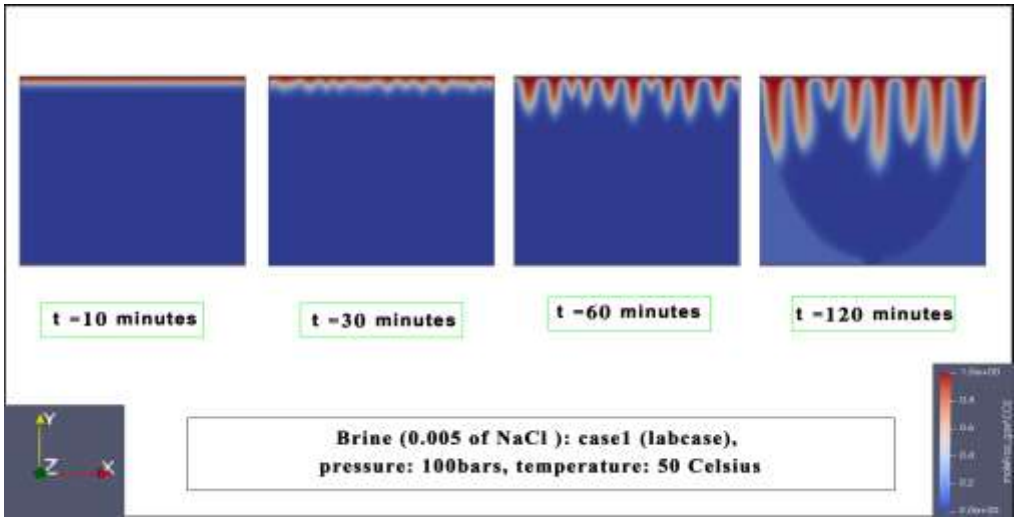

Figure(4.3.2). OPM-simulation result CO_2/brine(0.005 NaCl)-wet porous, permeability 76 Darcy

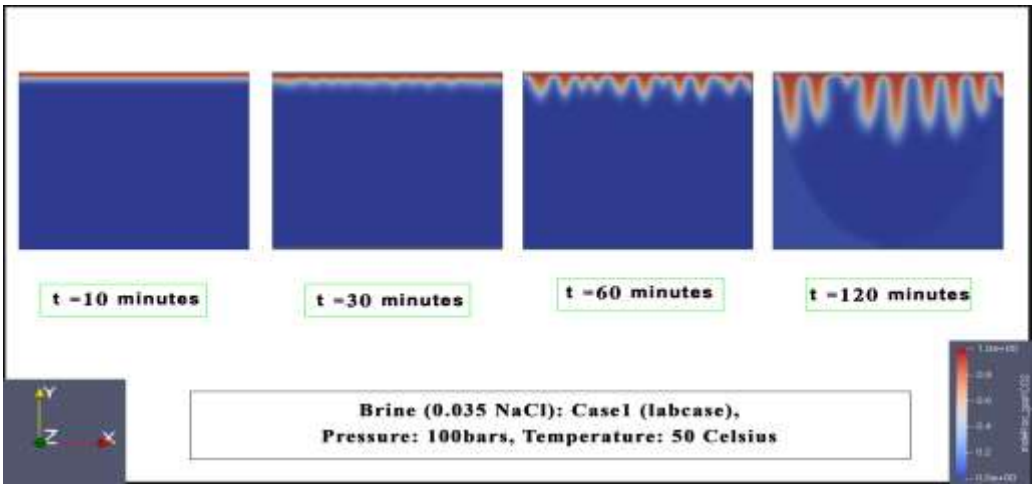

Figure(4.3.3). OPM-simulation result CO_2/brine(0.035 NaCl)-wet porous, permeability 76 Darcy

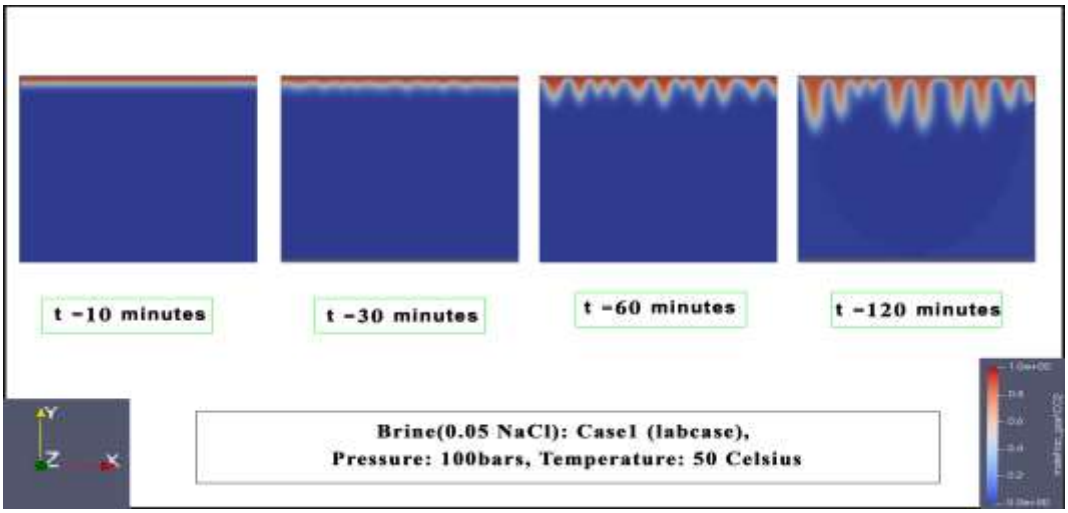

Figure(4.3.4). OPM-simulation result CO_2/brine(0.05 NaCl)-wet porous, permeability 76 Darcy

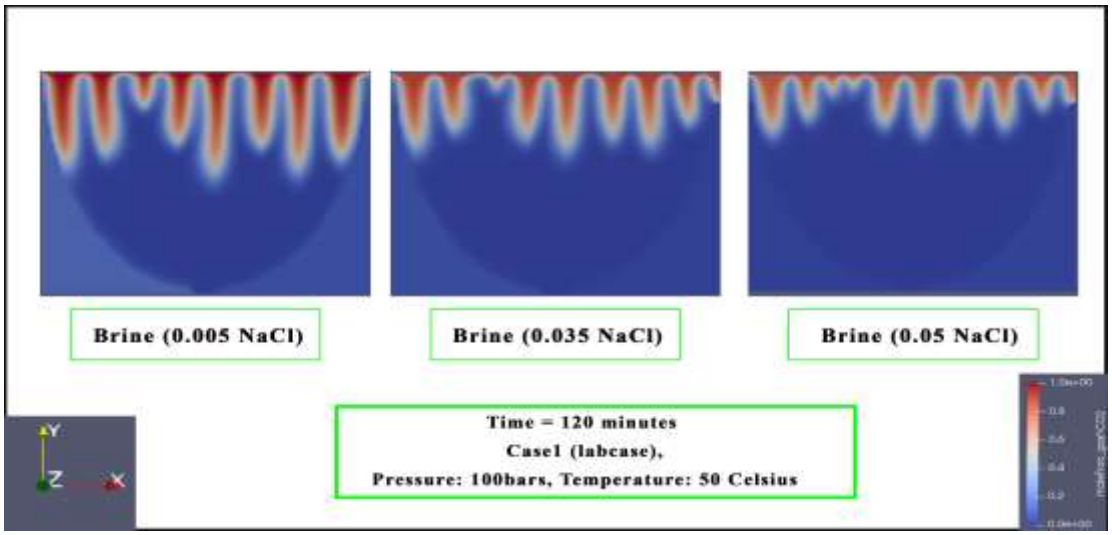

Figure(4.3.5). OPM-simulation result CO_2/brine(0.005, 0.035 and 0.05 NaCl)-wet porous, permeability 76 Darcy

Discussion results

Figure (4.3.1) shows the result of OPM-simulator for dissolution of carbon dioxide in pure water. From the time zero to 10 minutes was hard to observe any fingers, but we can observe growing of CO_2/pure water layers laterally, which occurs by the diffusion of carbon dioxide. Growing the fingers downwards are starting after 10 minutes and observed clearly at 30 minutes, because the thickness of water carbonate layers will increase sufficiently that will lead to gravitational instability. Therefore, the density-driven convection will occur. The density-driven is accelerating the dissolution of carbon dioxide in water. Therefore, the penetration of fingers is increasing by time (120 minutes).

When the salinity is increasing dissolution of carbon dioxide is decreasing (salt out effect). (See the figures (4.3.2), (4.3.3), (4.3.4)and (4.3.5)). When the salinity is increasing the developing the thickness of water carbonate layers takes longer time to be sufficient to create the gravitational instability. Thus, developing of fingers will be slower when we compare it with pure water.

According to the Eq (2.4.1) when the salinity is increasing the Rayleigh number is decreasing, because by increasing the salinity that leads to increase of viscosity μ and density of brine. Thus, $\Delta\rho$ will decrease (the density difference between the mixture of (CO_2 , brine) and the density of brine). When the Rayleigh number Ra is decreasing that indicates to less carbon dioxide will dissolve in brine.

Case2 (Surface) at (Pressure 10 bars and temperature is 20 Celsius)

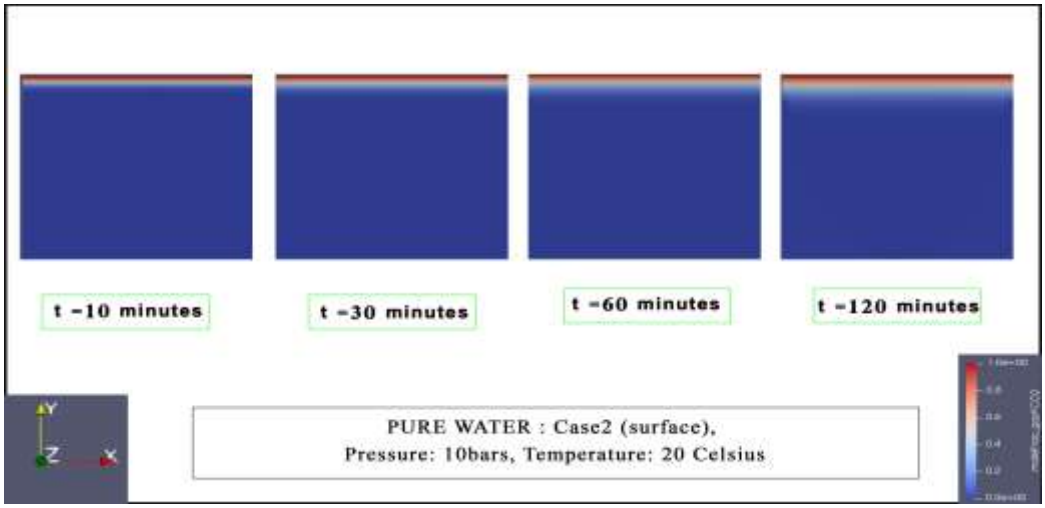

Figure(4.3.6). OPM-simulation result CO_2/pure water- wet porous, permeability 76 Darcy at (10 bars and 20 Celsius)

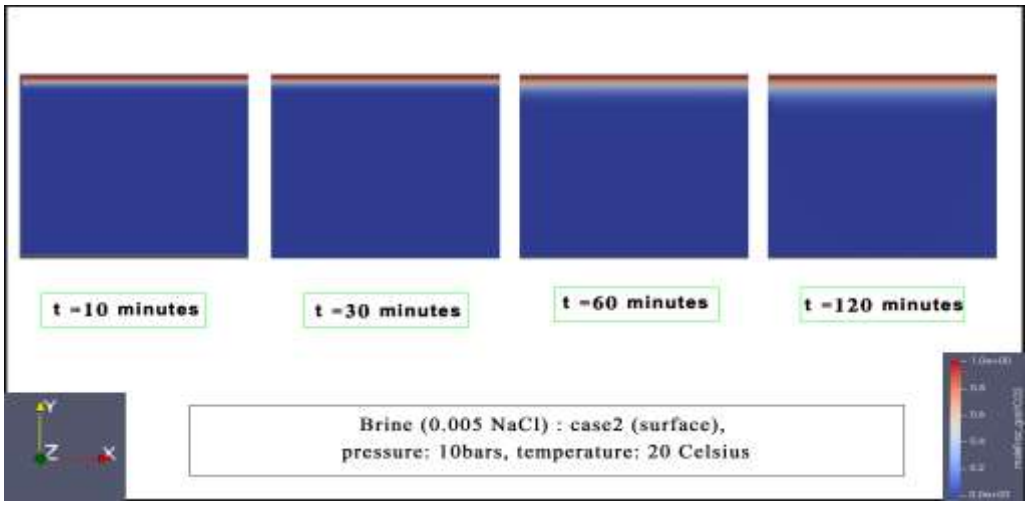

Figure(4.3.7). OPM-simulation result CO_2/brine(0.005 NaCl)- wet porous, permeability 76 Darcy at (10 bars and 2o Celsius)

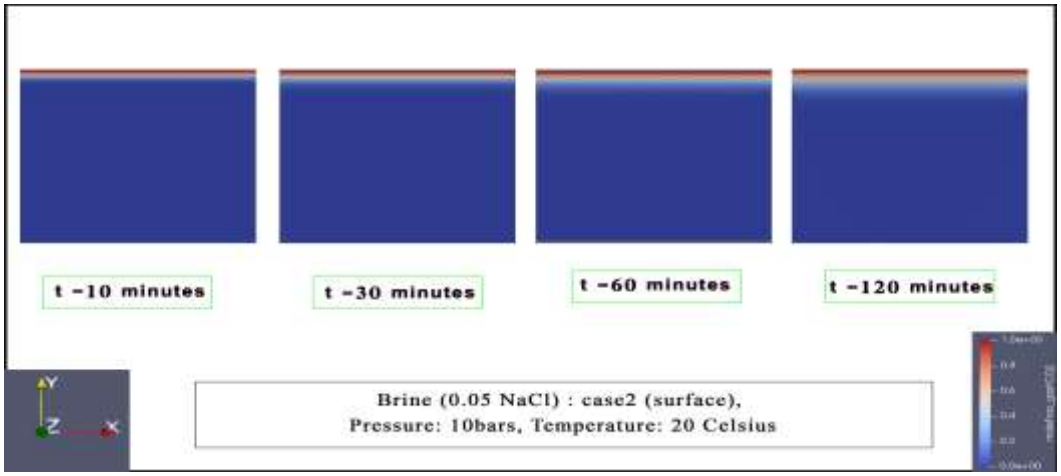

Figure(4.3.8). OPM-simulation result CO_2/brine(0.05 NaCl)- wet porous, permeability 76 Darcy at (10 bars and 2o Celsius)

In Case 2 the pressure is dropped to 10 bars. The pressure is critical factor on dissolution of carbon dioxide in water. The relation is direct proportion between pressure and dissolution of carbon dioxide. Therefore, the drop from 100 bars to 10 bars will reduce the dissolution of carbon dioxide significantly. The results of OPM-simulator show slow developing of water carbonate layers (see figure (4.3.7)) and the thickness of these layers are not enough to create gravitational instability. Therefore, was hard to observe any fingers in Case2. When the salinity is increasing in Case2 that will reduce more the developing of water carbonate layers (see the figures (4.3.7) and (4.3.8)). Therefore, observation of fingers will be much slower than pure water.

4-4: Results of OPM-simulator VS real experiment at same conditions for both Case1 and Case2.

In order to compare laboratory results with simulation results, simulation conditions must be made as close as possible to the conditions in which the experiment was performed in the laboratory. Case1 and Case 2 have been done experimentally also [4.4.1]. but at small scale , where the porous media was filled in pure water.

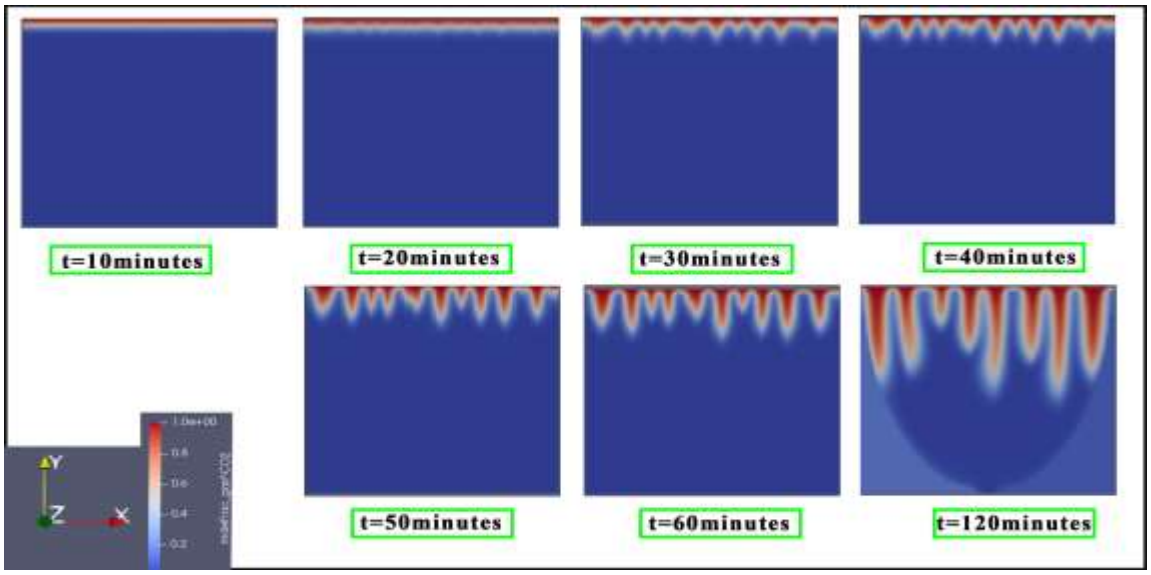

Figure(4.4.1). OPM-simulation results CO_2/pure water- wet porous, case1 (labcase) permeability 76 Darcy

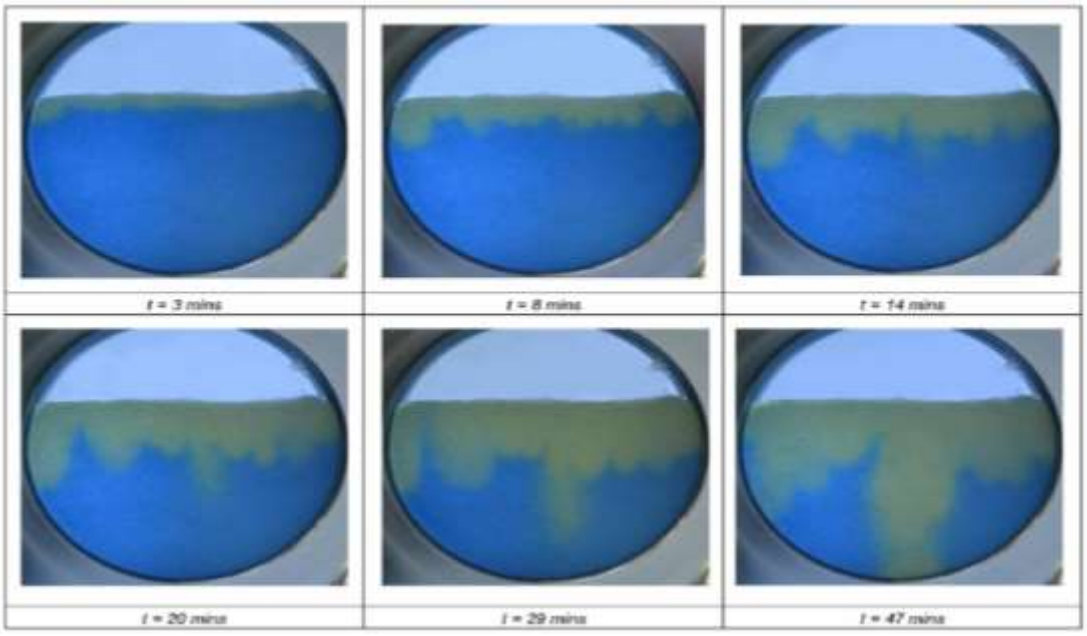

Figure(4.4.2). experiment results CO_2/pure water- wet porous, permeability 76 Darcy /pressure 100bars, Temperature 50 Celsius/ [4.4.1]

Figure (4.4.1) shows the simulation results, which shows the dissolution CO_2/pure water- wet porous, simulated by OPM-simulator for Case1 (labcase).

Figure (4.4.2) illustrates the developing of fingers in CO_2/pure water- wet porous experimentally[4.4.1].

Experimentally, developing of fingers in porous media are faster than simulation results. Figure(4.4.2) shows the appearing of fingers after 8 minutes, and it reaching the bottom of cell after 47 minutes. Figure (4.4.1) fingers are appearing after 20 minutes, the growth of these fingers is continuing but less frequently than experiment

Case 2 has been done experimentally also. Comparing the results of experiment (see the figure (4.4.4)) and simulation results (see figure (4.4.3)) also clearly show delaying between experiment's results and OPM-simulator's results as it illustrates.

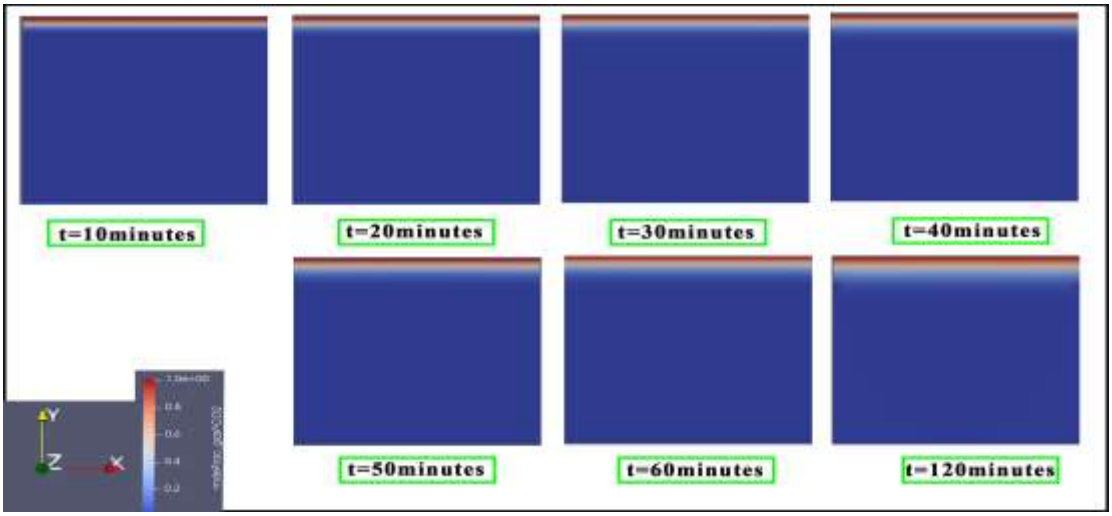

Figure(4.4.3). OPM-simulation results CO_2/pure water- wet porous, case2 (surface) permeability 76 Darcy

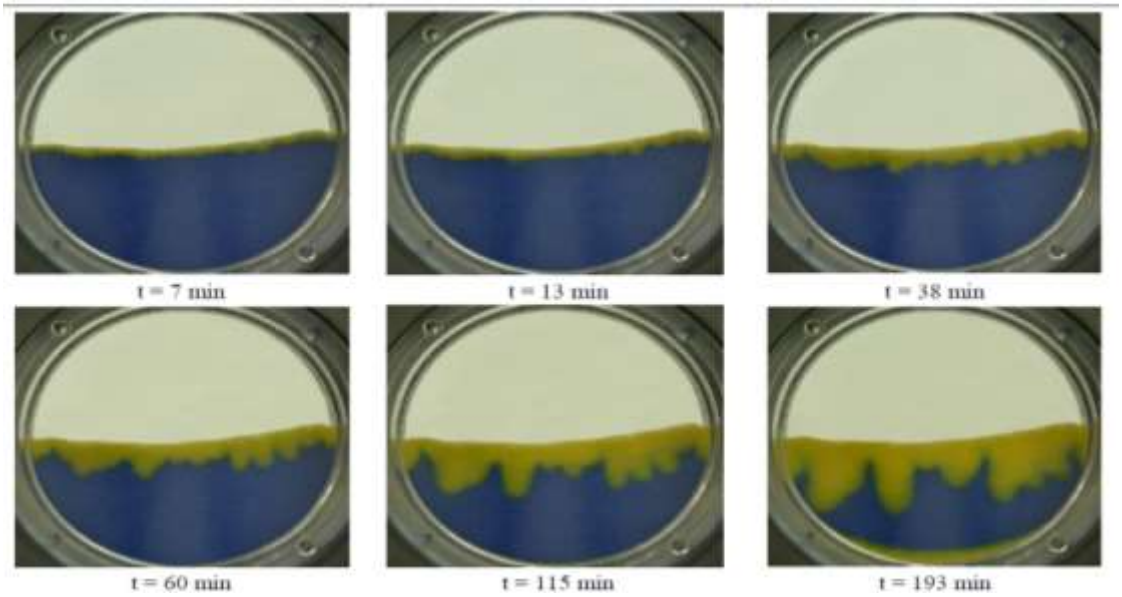

Figure(4.4.4). experiment results CO_2/pure water- wet porous, permeability 76 Darcy /pressure 10bares, Temperature 20 Celsius.

Figure (4.4.3) shows the dissolution of CO_2/pure water- wet porous, simulated by OPM-simulator for case2 (surface)

Figure (4.4.4) shows the developing of fingers in CO_2/pure water- wet porous experimentally[4.4.1].

Figure (4.4.3) doesn't show any developing of fingers as a result of the dissolution of carbon dioxide in pure water after 2 hours, because the pressure is dropped from 100 bars to 10 bars.

Figure (4.4.4) shows the developing of fingers clearly after 13 minutes.

We can say there is dallying between the experiment and simulation in both Case1 and Case 2, that can be for many reasons, some of them will be discussed below.

Discussion:

The OPM-simulator is showing the delaying of finger`s penetration in pure water- wet porous. That can be for many reasons:

1- In OPM-simulator is considering the diffusion coefficient as constant value, but the diffusion coefficient is time- dependent [4.4.2], [4.4.3].[4.4.4] increasing at early time (diffusion of gas) then it decreasing when the more carbon dioxide is dissolving in water (density-driven). According to the Eq (2.4.1)

$$Ra = \frac{K\Delta\rho gH}{\varphi\mu D}$$

When the diffusion coefficient is decreasing, Rayleigh number will increase. That means more carbon dioxide will dissolve

2- Packing the particles at the experiment can have some heterogeneity which will lead to have some capillary pressure or increment of permeability or error in the measuring the permeability its self.

3- The effect of viscosity :

Kumagai et al. (1998) measured the viscosity of water containing up to 4.8% (by weight) CO_2 at pressures up to 400 bar and the temperatures from 0° to 50° Celsius.

$$\mu_{H2O+Co2} = \mu_r * \mu_{H2O}$$

$$\mu_r = 1 + \frac{\sum_{i=1}^{2} a_i x_{CO_2}^i}{\sum_{i=0}^{1} b_i T^i}$$

Where is a, b Coefficients we can find them in tables x_{Co2} is CO_2 mass fraction.

The viscosity is increasing by dissolving of carbon dioxide in water.

OPM-simulator does not include the effect of changing of viscosity on the CO_2 dissolution. According to the Eq (2.4.1)

The relation between Rayleigh number and viscosity is inverse proportion; therefore, increasing of viscosity will lead to decrease of Rayleigh number. Thus, decreasing of the dissolution of carbon dioxide in water, but at same time will increase the $\Delta\rho$ will increase. Thus, we can say that the effect of the viscosity change on the insolubility will be small.

4.5 The effect of permeability on the transportation of carbon dioxide in water.

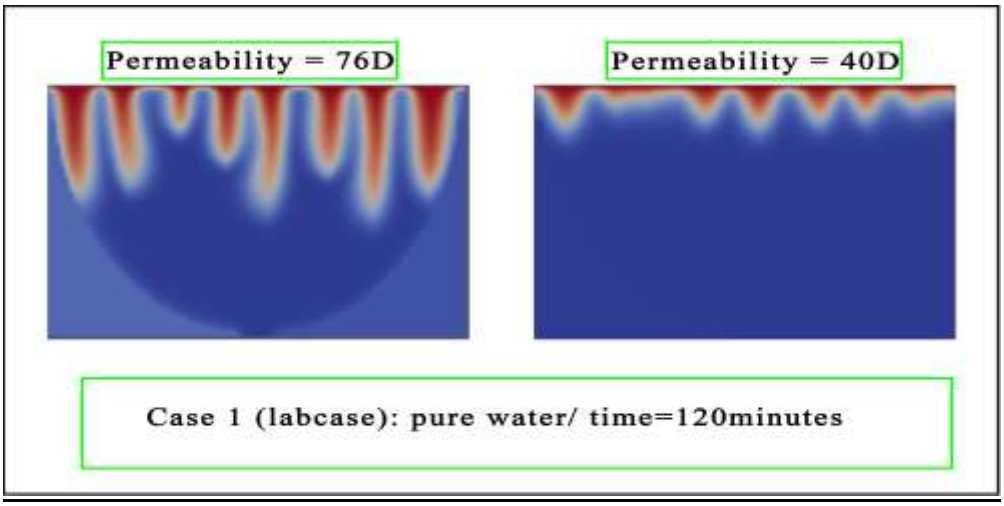

Figure(4.5.1). OPM-simulation results CO_2/pure water- wet porous, case1 (labecase)

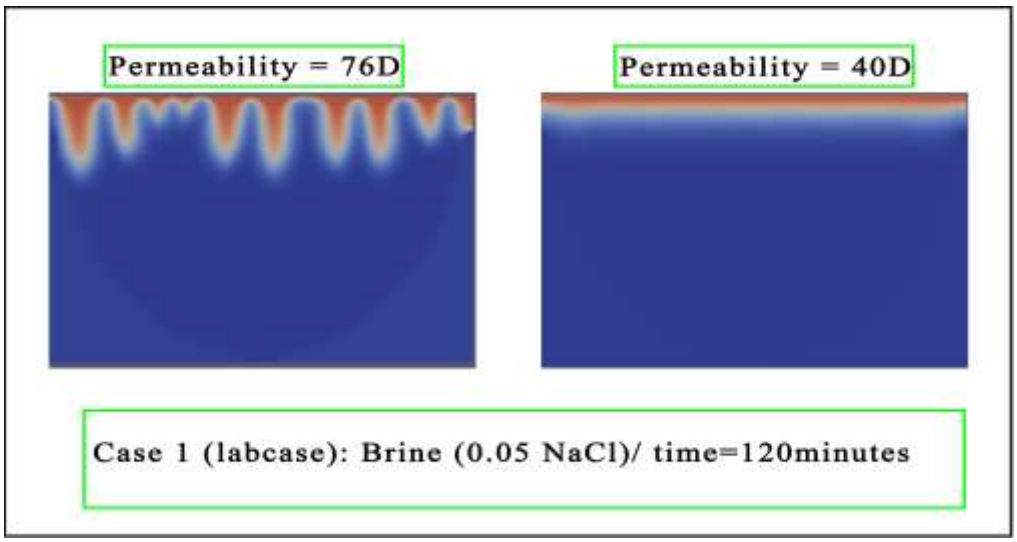

Figure(4.5.2). OPM-simulation results CO_2/brine (0.05 NaCl)- wet porous, case1 (labecase)

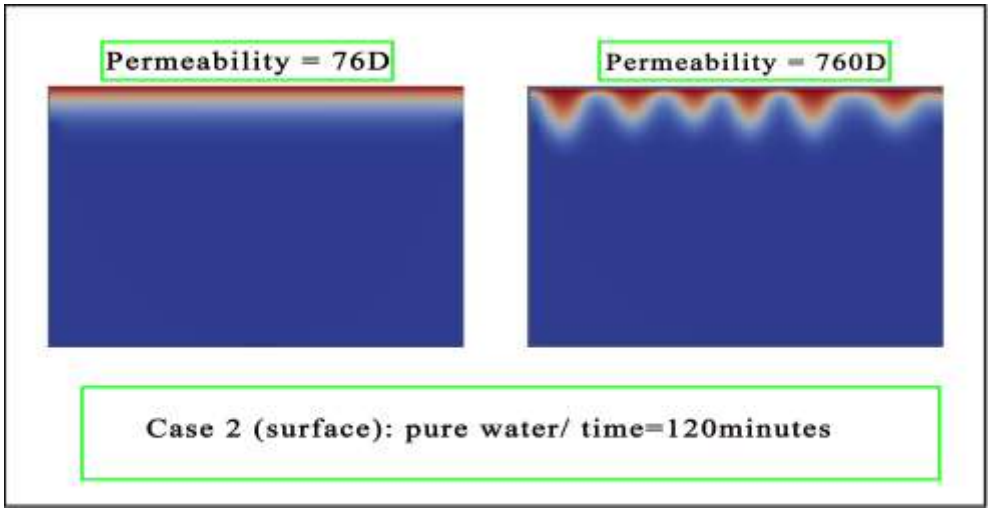

Figure(4.5.3). OPM-simulation results CO_2/pure water- wet porous, case2 (surface)

Figures (4.5.1) and (4.5.2): are illustrating the effect of changing the permeability from 76 Darcy to 40 Darcy on the dissolution of CO_2 in pure water and brine (0.05 NaCl) respectively at 2 hours by using OPM-simulator.

Decreasing the permeability caused the sharp decreasing in the dissolution of carbon dioxide in water.

Figure (4.5.3) is illustrating the effect of increasing the permeability from 76 Darcy to 760 Darcy on the dissolution of CO_2 in pure water at Case 2 (surface) at 2 hours by using OPM-simulator. Increasing the permeability is leading to significant increment of dissolution of carbon dioxide in water.

Discussion:

According to the Eq (2.4.1)

There is direct proportion between the permeability K and Rayleigh number R_a, therefore decreasing the permeability will lead to decrease of Rayleigh number , thus decreasing the dissolution of carbon dioxide. And increasing the permeability will lead to increase the Rayleigh number, thus increment in dissolution CO_2.

4.6 impact the diffusion coefficient D on the dissolution of carbon dioxide.

First, when diffusion coefficient is increasing :

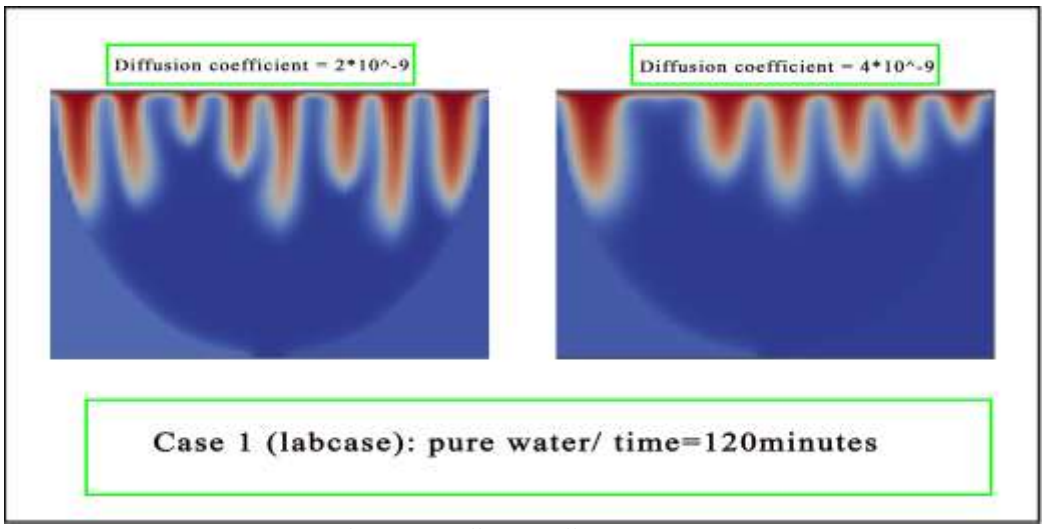

Figure(4.6.1). OPM-simulation results of increasing diffusion coefficient on CO_2/pure water- wet porous, case1 (labecase)

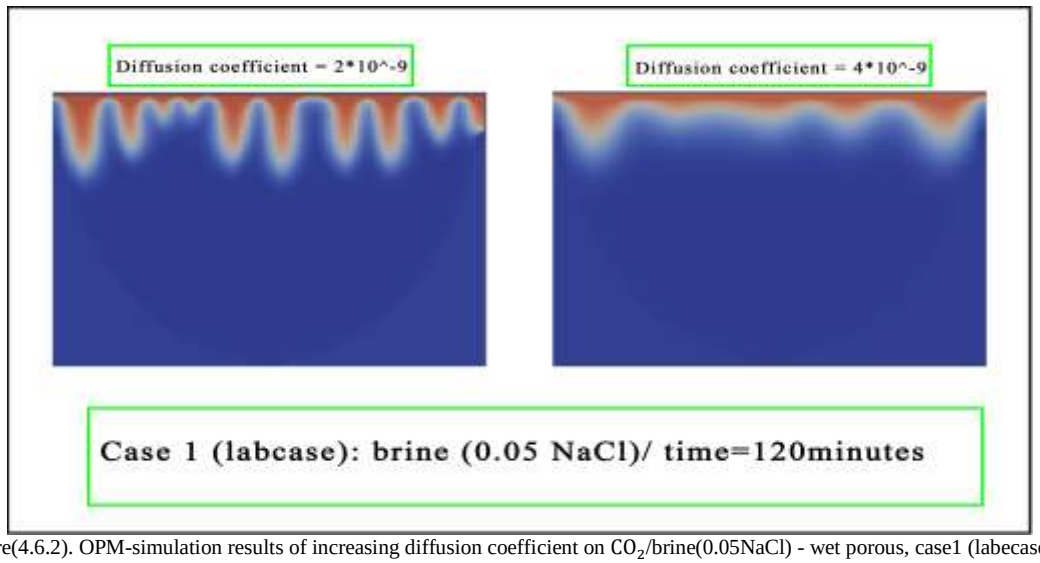

Figure(4.6.2). OPM-simulation results of increasing diffusion coefficient on CO_2/brine(0.05NaCl) - wet porous, case1 (labecase)

Figures (4.6.1): is showing the effect of increasing of diffusion coefficient on CO_2 dissolution rate in pure water-wet porous (case1) which has permeability 76 D after 120 minutes by using OPM-simulator. The diffusion coefficient increased from $2*10^{-9}$ to $4*10^{-9}$ $\frac{m^2}{s}$ after 120 minutes.

Figures (4.6.2): is showing the effect of increasing of diffusion coefficient on CO_2 dissolution in brine (0.05 NaCl)-wet porous (case1) which has permeability 76 D after 120 minutes by

using OPM-simulator. The diffusion coefficient increased from $2*10^{-9}$ to $4*10^{-9}\ \frac{m^2}{s}$ after 120 minutes. Both figures show when the diffusion coefficient is increased, that leads reduction of CO_2 dissolution in both pure water and brine which contains (0.05 NaCl).

Discussion:

According to Rayleigh number equation Eq (2.4.1), there is inverse proportion between diffusion coefficient and Rayleigh number. By increasing the diffusion coefficient, Rayleigh number will decrease and that will lead to reduce (density-driven convection).

Second, when the diffusion coefficient is decreased

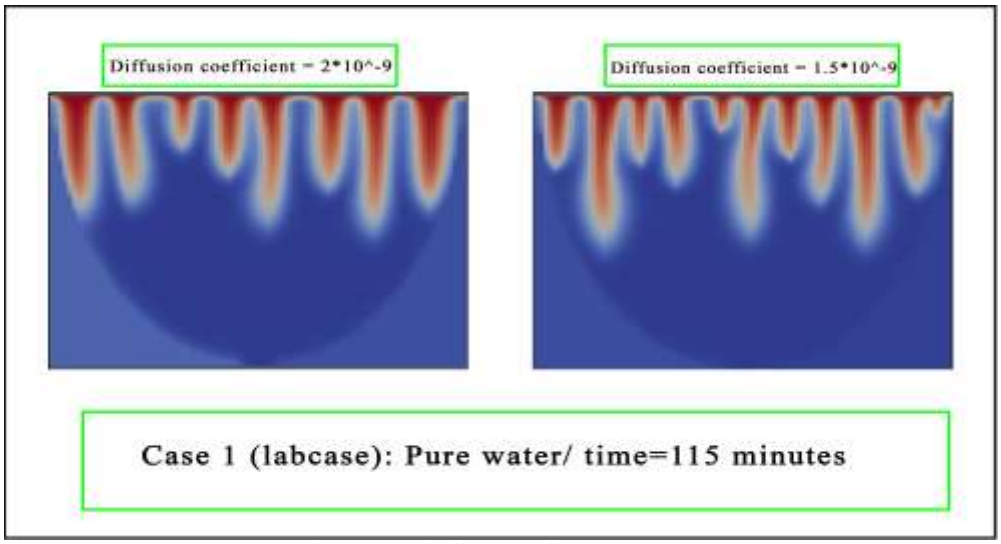

Figure(4.6.3). OPM-simulation results of reduction of diffusion coefficient on CO_2/pure water- wet porous, case1 (labecase)

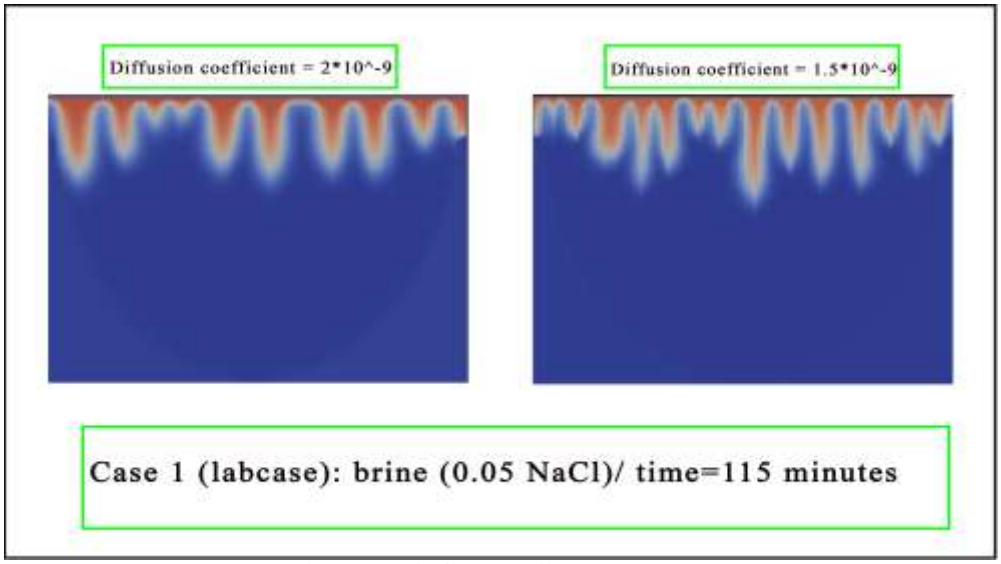

Figure(4.6.4). OPM-simulation results of reduction of diffusion coefficient on CO_2/brine (NaCl)- wet porous, case1 (labecase)

Figures (4.6.3): is showing the effect of reduction of diffusion coefficient on CO_2 dissolution in pure water-wet porous which has permeability 76 D after 115 minutes by using OPM-simulator.

Figures (4.6.4): is showing the effect of reduction of diffusion coefficient on CO_2 dissolution in brine (0.05 NaCl)-wet porous which has permeability 76 D after 115 minutes by using OPM-simulator. The diffusion coefficient reduced from $2*10^{-9}$ to $1.5*10^{-9}\ \frac{m^2}{s}$ after 115 minutes. Both figures show when the diffusion coefficient is reduced, that leads to increase the density-driven convection.

Discussion:

According to Rayleigh number equation Eq (2.4.1), there is inverse proportion between diffusion coefficient and Rayleigh number. By decreasing the diffusion coefficient, Rayleigh number will increase and that will lead to increase CO_2 dissolution (density-driven convection).

4.7 The effect of permeability heterogeneity on CO_2 dissolution rate

At real storage sites where carbon dioxide will be injected mostly have heterogeneous porous media; therefore simulating CO_2 dissolution in heterogeneous pores will give us better understanding the impact of heterogeneity of CO_2 dissolution pure water and brines. In this part the impact of heterogeneity will be illustrated in small/scale.

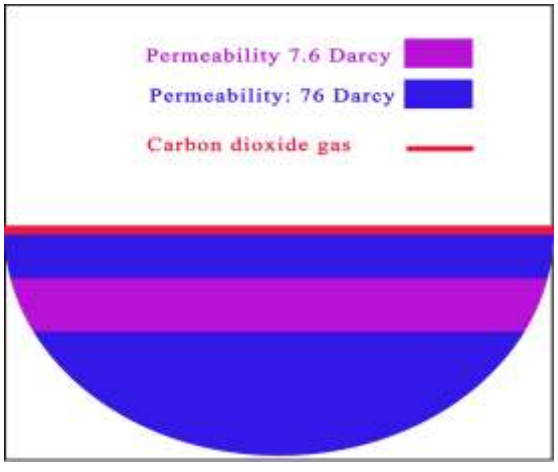

Figure (4.7.1) schematic drawing shows the horizontal low permeability layer layer

Figure (4.7.1) is schematic drawing of the location of horizontal low permeability layer, which disturbs the homogeneity of porous media. This layer has lower permeability that main porous media.

OPM-simulator will be used to simulate the dissolution of carbon dioxide in this new porous structure.

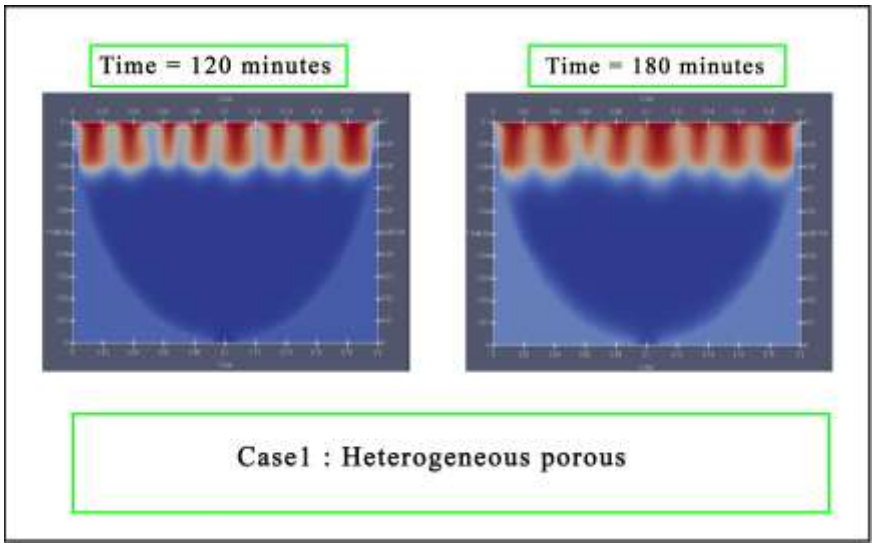

Figure (4.7.2) OPM-simulation results/ case1/effect of heterogeneity on CO_2 dissolution vs time

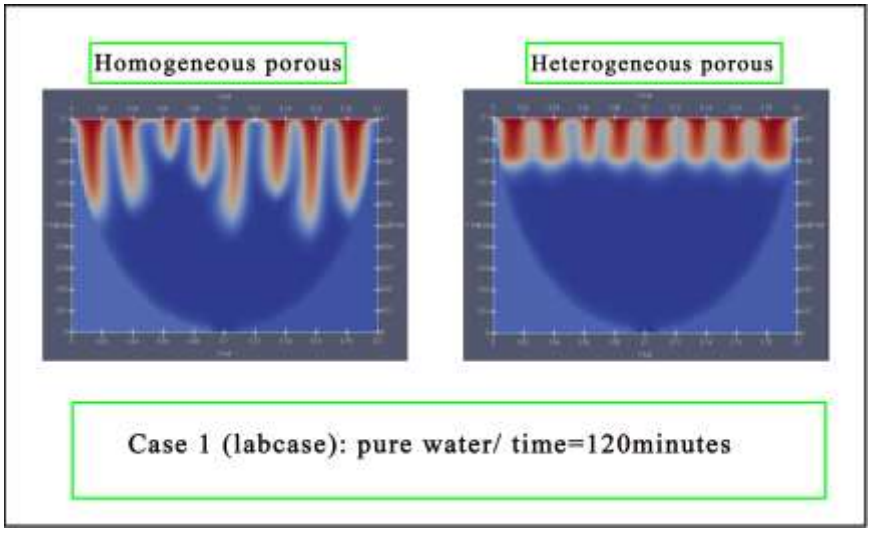

Figure (4.7.3) OPM-simulation results/ case1/effect of heterogeneity on CO_2 dissolution vs time

Figure (4.7.2) is illustrating the impact of permeability heterogeneity on the transportation of carbon dioxide in porous media. When the low permeability layer is interrupting the track of carbon dioxide, this layer works as barrier for the transportation CO_2, as it discussed in part (4.5) impact permeability on the CO_2 dissolution. The rate of penetration of fingers is very slow after 3 hours, but at same time the diffusion is helping to dissolve more carbon dioxide laterally.
Figure(4.7.3) is showing the comparing of CO_2 dissolution rate between homogeneous porous media which has 76 D and heterogeneous porous media which interrupted by lower permeability layer 7.6 Darcy.
OPM-simulator results are illustrating that the CO_2 dissolution is higher in homogenous porous media than heterogeneous porous.

Chapter 5

5.1 general discussions

OPM-simulator shows the ability to simulate the CO_2 dissolution in porous media, which contains pure water or brine with different concentrations of salinity for different cases (Case1 and Case2).

OPM-simulator gives a realistic view about the carbon dioxide solubility and the effect of factors that affecting on the solubility, despite the results of laboratory experiments and simulation output shows delaying, which dissolution is faster in experiment than simulation.

Conducting laboratory experiments and collecting the correct data, and considering them in the OPM-simulator, that will help to improve the results of the simulation and bringing them closer to the laboratory results.

When reaching convergence in laboratory and simulation results, OPM-simulator can be adopted in practical projects. In this way, time, effort and money can be saved. Because lab experiments take a lot of money and time.

5.2 further steps can be done on OPM-simulator.

1- Real geological sites will contain different minerals such as Fe, Ca and Mg therefore studying the impact of minerals on the CO_2 dissolution can be studied by OPM-simulator.
2- Simulating CO_2 dissolution in oil phase is helpful for EOR projects.
3-using OPM-simulator to study the transportation of carbon dioxide in emulsified (water-oil) phase.
4- Simulating CO_2 dissolution in complex heterogeneous porous media, that by adding horizontal, vertical and diagonal layers with different permeability.

5.3 Restrictions of OPM results

1. The difficulty of working on OPM-simulator, especially for people who are not familiar with Linux system.
2. The tables which are used in OPM-simulator do not contain sufficient explanation, which makes it difficult to understand by other users.
3. The difficulty of the OPM's response to changing some values, which make us restricted to specific values. Here are some restrictions during the studying of CO_2 dissolution.

   a. during the studying of impact of diffusion coefficient, was hard to reduce it below $1.5 * 10^{-9} \frac{m^2}{s}$ and max time for simulation was 115 minutes (4.6).

   b. the quality of tables: some tables were easy to build and flexibility was good for changing the values, for instance all salinity tables were easier to build that pure water in both cases (case1 and case2).

c. Difficulty to determine the physical time on (Para view) program, because it is showing it as time steps.

5.4 developing of OPM-simulator

a. Possibility to change the parameters like Pressure, Temperature, permeability etc direct from ParaView.
b. Possibility to see the physical time on Para View, not only as time steps.
c. Possibility to merge the files an illustrating the effect of this merge direct on ParaView.

References

[a.1]Keith, D.W., Hassanzadeh, H., Pooladi-Darvish, M., 2005. Reservoir engineering to accelerate dissolution of stored CO2 in brines. In: Proceedings of the Seventh International Conference on Greenhouse Gas Control Technologies (GHGT-7), Vancouver, Canada

[1.1]Whitson CH, BrulΘ MR (2000) Phase behavior. Society of Petroleum Engineer, Richardson

[a.2] Leonenko, Y., Keith, D.W., Pooladi-Darvish, M., Hassanzadeh, H., 2006. Accelerating the dissolution of CO2 in aquifers. In: Proceedings of the Eighth International Conference on Greenhouse Gas Control Technologies (GHGT-8), Trondheim, Norway.

[a.3]Taku Ide, S., Jessen, K., Orr Jr., F.M., 2007. Storage of CO2 in saline aquifers: effects of gravity, viscous, and capillary forces on amount and timing of trapping. Int. J. Greenh. Gas Control 1 (4), 481–491.

[a.4]Leonenko, Y., Keith, D.W., 2008. Reservoir engineering to accelerate the dissolution of CO2 stored in aquifers. Environ. Sci. Technol. 42 (8), 2742–2747.

[a.5]Hassanzadeh, H., Pooladi-Darvish, M., Keith, D.W., 2009a. Accelerating CO2 dissolution in saline aquifers for geological storage – mechanistic and sensitivity studies. Energy Fuels 23 (6), 3328–3336

[2.1] Perkins E (2003) Fundamental geochemical processes between CO_2, water and minerals. Alberta Innovates–Technology Futures
Qu X, Lei Q, He Y, Chen Z, Yu H (2018) Experimental investigation of the EOR performances of carbonated water injection in tight sandstone oil reservoirs. Earth Environ Sci 208:12054

[1.2.1] Bamberger A, Sieder G, Maurer G (2000) High-pressure (vapor-liquid) equilibrium in binary mixtures of (carbon dioxide + water or acetic acid) at temperatures from 313 to 353 K. J Supercrit Fluids 17(2):97–110

[1.2.2] Chang Y-B, Coats BK, Nolen JS (1998) A compositional model for CO2 floods including CO2 solubility in water. SPE Reservoir Eval Eng 1(2):155–160

[1.2.3] Chapoy A, Mohammadi A, Chareton A, Tohidi B, Richon D (2004) Measurement and modeling of gas solubility and literature review of the properties for the carbon dioxide–water system. Ind Eng Chem Res 43(7):1794–1802.

[1.2.4] Gui X, Wang W, Gao Q, Yun Z, Fan M, Chen Z (2017) Measurement and correlation of high pressure phase equilibria for CO2 + alkanes and CO2 + crude oil systems. J Chem Eng Data 62(11):3807–3822

[1.2.5]Liu Y, Hou M, Yang G, Han B (2011) Solubility of CO2 in aqueous solutions of NaCl, KCl, CaCl2 and their mixed salts at different temperatures and pressures. J Supercrit Fluids 56(2):125–129

[1.2.6]Valtz A, Chapoy A, Coquelet C, Paricaud P, Richon D (2004) Vapourliquid equilibria in the carbon dioxide-water system, measurement and modelling from 278.2 to 318.2 K. Fluid Phase Equilib 226:333–344

[1.2.7]Duan Z, Sun R, Zhu C, Chou IM (2006) An improved model for the calculation of CO2 solubility in aqueous solutions containing Na+, K+,Ca2+,Mg2+,Cl−,and SO42−. Mar Chem 98(2–4):131–139

[1.2.8]Mao S, Duan Z, Hu J, Zhang D (2010) A model for single-phase PVTx properties of CO2–CH4–C2H6–N2–H2O–NaCl fluid mixtures

from 273 to 1273 K and from 1 to 5000 bar. Chem Geol
275(3–4):148–160.

[1.2.9] Enick RM, Klara SM (1990) CO2solubility in water and brine under
reservoir conditions. Chem Eng Commun 90(1):23–33.

[1.3.1] Diamond LW, Akinfiev NN (2003) Solubility of CO2
in water from1.5 to 100 C and from 0.1 to 100 MPa: evaluation of literature
data and thermodynamic modelling. Fluid Phase Equilib
208(1–2):265–290

[1.3.2] Kechut NI, Sohrabi M, Jamiolahmady M (2011) Experimental and
numerical evaluation of carbonated water injection (CWI) forimproved oil recovery and CO2
storage. SPE-143005

[1.3.3] Perkins E (2003) Fundamental geochemical processes between CO2,
water and minerals. Alberta Innovates–Technology Futures.

[1.3.4] Chang Y-B, Coats BK, Nolen JS (1998) A compositional model for
CO_2 floods including CO_2 solubility in water. SPE Reservoir Eval
Eng 1(2):155–160

[1.4.1] Fick's law was formulated by the German physiologist Adolf Eugen Fick (1829–1901) in 1855.

[1.4.2] Hassanzadeh, H., Pooladi-Darvish, M. & Keith, D.W. (2006). Stability of a fluid in a horizontal saturated porous layer: Effect of non-linear concentration profile, initial, and boundary conditions. *Transport in Porous Media, 65*(2), 193-211. doi: https://doi.org/10.1007/s11242-005-6088-1.

[1.4.3] Lindeberg, E. & Wessel-Berg, D. (1997). Vertical convection in an aquifer column under a gas cap of CO2. *Energy Conversion and Management, 38*(supplement) 229-234. doi: https://doi.org/10.1016/S0196-8904(96)00274-9.

[1.4.4] Ennis-King, J. & Paterson. L. (2005). Role of Convective Mixing in the Long-Term Storage of Carbon Dioxide in Deep Saline Formations. *Society of Petroleum Engineers, 10*(3), 349-356. doi: https://doi.org/10.2118/84344-PA.

[1.4.5] Emami-Meybodi, H., Hassanzadeh, H., Green, C.P. & Ennis-King, J. (2015). Convective dissolution of CO2 in saline aquifers: Progress in modeling and experiments. *International Journal of Greenhouse Gas Control, 40*(2015). 238-266. doi: https://doi.org/10.1016/j.ijggc.2015.04.003.

[1.4.6] Lindeberg, E. & Wessel-Berg, D. (2011). Upscaling studies of diffusion induced convection in homogeneous and heterogeneous aquifers. *Energy Procedia, 4*(2011), 3927-3934. doi: https://doi.org/10.1016/j.egypro.2011.02.331.

[1.4.7] Pau, G.S.H., Bell, J.B., Pruess, K., Almgren, A.S., Lijewski, M.J. & Zhang, K. (2010). High-resolution simulation and characterization of density-driven flow in CO2 storage in saline aquifers. *Advances in Water Resources, 33*(4). 443-455. doi: https://doi.org/10.1016/j.advwatres.2010.01.009.

[1.4.8] Ennis-King, J. & Paterson. L. (2005). Role of Convective Mixing in the Long-Term Storage of Carbon Dioxide in Deep Saline Formations. *Society of Petroleum Engineers, 10*(3), 349-356. doi: https://doi.org/10.2118/84344-PA

[1.4.9] Faisal, T.F., Chevalier, S., Bernabe, Y., Juanes, R. & Sassi, M. (2015). Quantitative & qualitative study of density driven CO2 mass transfer in a vertical Hele-Shaw cell. *International Journal of Heat and Mass Transfer, 81*(2015). 901-914. doi: https://doi-org /10.1016/j.ijheatmasstransfer.2014.11.017

[1.4.10] Kneafsey, T.J. & Pruess, K. (2010). Laboratory Flow Experiments for Visualizing Carbon Dioxide-Induced, Density-Driven Brine Convection. *Transport in Porous Media, 82*(1), 123-139. doi: https://doi.org/10.1007/s11242-009-9482-2

[2.2.1] Gross PM. The "Salting out" of Nonelectrolytes from Aqueous Solutions. Chemical Reviews. 1933 August; 13(1).

[2.3.1] , Czernichowski-Lauriol, I., Pruess, K., Xu, T., 2007. Two-dimensional reactive transport modeling of CO2 injection in a saline aquifer at the Sleipner site,North Sea. Am. J. Sci. 307, 974–1008. doi:10.2475/07.2007.02

[2.3.2] Bowker KA, Shuler PJ (1991) Carbon dioxide injection and resultant alteration of the Weber Sandstone, Rangely Field, Colorado. AAPG Bull 75(9):1489–1499

[2.3.3] Grigg RB, Svec RK (2006) CO2 transport mechanisms in CO2/ brine core flooding. SPE-103228 Gui X, Wang W, Gao Q, Yun Z, Fan M, Chen Z (2017) Measu

[2.3.4] Shiraki R, Dunn TL (2000) Experimental study on water–rock interactions during CO2 flooding in the Tensleep Formation, Wyoming, USA. Appl Geochem 15(3):265–279

[2.3.5] Wellman TP, Grigg RB, McPherson BJ, Svec RK, Lichtner PC (2003) Evaluation of CO2- brine-reservoir rock interaction with laboratory flow tests and reactive transport modeling. SPE-80228

[2.3.6] Izgec O, Demiral B, Bertin H, Akin S (2008) CO2 injection into saline carbonate aquifer formations I: laboratory investigation. Transp Porous Media 72(1):1–24

[2.3.7] Sayegh SG, Krause FF, Girard M, DeBree C (1990) Rock/fluid interactions of carbonated brines in a sandstone reservoir: Pembina Cardium, Alberta, Canada. SPE Form Eval 5(4):399–405

[2.3.8] Kono F, Kato A, Shimokawara M, Tsushima K (2014) Laboratory measurements on changes in carbonate rock properties due to CO2-saturated water injection. SPE-172013

[2.4.1] Emami-Meybodi, H. Stability analysis of dissolution-driven convection in porous media. Phys. Fluids 2017, 29, No. 014102.

[2.4.2] Emami-Meybodi, H.; Hassanzadeh, H. Two-phase convective mixing under a buoyant plume of CO2 in deep saline aquifers. Adv. Water Resour. 2015, 76, 55−71.

[2.4.3] Khosrokhavar, R., Elsinga, G., Farajzadeh, R. & Bruining, H. (2014). Visualization and investigation of natural convection flow of CO2 in aqueous and oleic systems. Journal of Petroleum Science and Engineering, 122(2014), 230-239. doi: https://doi.org/10.1016/j.petrol.2014.07.016

[2.4.4] Farajzadeh, R., Ranganathan, P., Zitha, P.L.J. & Bruining J. (2011). The effect of heterogeneity on the character of density-driven natural convection of CO2 overlying a brine layer. *Advances in Water Resources, 34*(3), 327-339. doi: https://doi-org /10.1016/j.advwatres.2010.12.012.

[2.4.5] Slim, C. A.; Bandi, M. M.; Miller, C. J.; et al. Dissolution-driven convection in a Hele-Shaw cell. Phys. Fluids 2013, 25, 024101.

[2.4.6] Faisal, T. F.; Chevalier, S.; Bernabe, Y.; et al. Quantitative and qualitative study of density driven CO2 mass transfer in a vertical

[2.4.7] Ennis-King, J. P.; Paterson, L. Role of Convective Mixing in the Long-Term Storage of Carbon Dioxide in Deep Saline Formations. SPE Journal 2013, 10, 349−356.

[2.4.8] Nield, D. A. Onset of Thermohaline Convection in a Porous Medium. Water Resour. Res. 1968, 4, 553−560.

[2.4.9] Slim, A. C.; Ramakrishnan, T. S. Onset and cessation of timedependent, dissolution-driven convection in porous media. Phys. Fluids 2010, 22, 124103.

[2.4.10] Szulczewski, M. L.; Hesse, M. A.; Juanes, R. Carbon dioxide dissolution in structural and stratigraphic traps. J. Fluid Mech. 2013, 736, 287−315.

[2.4.11] Slim, A. C. Solutal-convection regimes in a two-dimensional porous medium. J. Fluid Mech. 2014, 741, 461−491.

[2.4.12] Hassanzadeh, H.; Pooladi-Darvish, M.; Keith, D. W. Scaling behavior of convective mixing, with application to geological storage of CO2. AIChE J. 2007, 53, 1121−1131.

[2.4.19] Teng, Y.; Jiang, L.; Fan, Y.; et al. Quantifying the dynamic density driven convection in high permeability packed beds. Magn. Reson. Imaging 2017, 39, 168−174.

[2.4.13] Lindeberg, E.; Wessel-Berg, D. Upscaling studies of diffusion induced convection in homogeneous and heterogeneous aquifers. Energy Procedia 2011, 4, 3927−3934.

[2.4.14] Farajzadeh, R.; Salimi, H.; Zitha, P. L. J.; et al. Numerical Simulation of Density-Driven Natural Convection in Porous Media with Application for CO2 Injection Projects. Int. J. Heat Mass Transfer 2007, 50, 5054−5064.

[2.5.1] Arrhenius, S. A. (1889). "Über die Dissociationswärme und den Einfluß der Temperatur auf den Dissociationsgrad der Elektrolyte" (PDF). *Z. Phys. Chem.* **4**: 96–116. doi:10.1515/zpch-1889-0408.

[2.5.2] Arrhenius, S. A. (1889). "Über die Reaktionsgeschwindigkeit bei der Inversion von Rohrzucker durch Säuren". *Z. Phys. Chem.* 4: 226–48. doi:10.1515/zpch-1889-0116.

[2.5.3] Farajzadeh, R., Barati, A., Delil, H.A., Bruining, J. & Zitha, P.L.J. (2007). Mass Transfer of CO2 Into Water and Surfactant Solutions. *Petroleum Science and Technology, 25*(12). 1493-1511. doi: https://doi-org /10.1080/10916460701429498.

[3.1.0] Stocker, T.F., Qin, D., Plattner, G.-K., Tignor, M., Allen, S.K., Boschung, J., Nauels, A., Xia, Y., Bex, V., Midgley, P.M., 2013. IPCC, CLimate Change 2013: The Physical Science Basis. Contribution of Working Group I to the Fifth Assessment Report of the Intergovernmental Panel on Climate Change. Clim. Chang. 2013 5, 1535.

[3.1.1] Edenhofer, O., Pichs-Madruga, R., Sokona, Y., Farahani, E., Kadner, S., Seyboth, K., Adler,A., Baum, I., Brunner, S., Eickemeier, P., Kriemann, B., Savolainen, J., Schlimer, S., von Stechow, C., Zwickel, T., Minx, J.C., others, Schlümer, S., von Stechow, C., Zwickel, T., Minx, J.C., 2014. IPCC, Climate Change 2014: Mitigation of Climate Change. Cambridge University Press.

[3.1.2] Metz, B., Davidson, O., De Coninck, H., Loos, M., and Meyer, L. (2005). IPCC special report on carbon dioxide capture and storage: Prepared by working group III of the intergovernmental panel on climate change. IPCC, Cambridge University Press: Cambridge, United Kingdom and New York, USA, 2.

[3.2.1] IPCC, IPCC Special Report on Carbon Dioxide Capture and Storage, Cambridge University Press, Cambridge, 2005.

[3.2.2] Johnsson, F., Perspectives on CO2 capture and storage.

Greenhouse Gas Sci. Technol., 2011, **1**, 119–133.

[3.3.1] Scientific facts on CO2 capture and storage – GreenFacts; www.greenfacts.org/en/co2-capture-storage/

[5.1.1] Bachu, S., Gunter, W. D. and Perkins, E. H., Aquifer disposal of CO2: Hydrodynamic and mineral trapping. *Energ. Convers. Manage.*, 1994, **35**, 269–279.

[3.5.2] Tzimas, E., Georgakaki, A., Garcia Cortes, C. and Peteves, S. D., Possibilties for enhanced oil recovery using carbon dioxide in the European Energy System. In Proceedings of the 8th International Conference on Greenhouse Gas Control Technologies, Trondheim, Norway, 2006.

[3.5.3] . Kumar, B., Issues for carbon dioxide storage in India, Presentation at the International Workshop on Carbon Capture and Storage in the Power Sector: R&D Priorities for India, New Delhi, 2008.

[3.5.4] Jackson, G., CO2 enhancement of methane production and reduction of water in high permeability, undersaturated coal seams – a modelling study. In Proceedings of the 8th International Conference on Greenhouse Gas Control Technologies, Trondheim, Norway, 2006.

[3.6.1] Bradshaw J, Bachu S, Bonijoly D, Burruss R, Holloway S, Christensen NP,

et al. CO2 storage capacity estimation:
Issues and development of standards.
International Journal of Greenhouse Gas
Control. 2007;**1**:62-68

[3.6.2] Carbon Sequestration Leadership
Forum (CSLF). Phase I Final Report
from the Task Force for Review and
Identification of Standards for CO2 Storage Capacity Measurement,
CSLF-T-2005-9 15. Berlin, Germany;
2005. p. 16

[3.6.3] Carbon Sequestration Leadership
Forum (CSLF). Phase II Final Report
from the Task Force for Review
and Identification of Standards for
CO2 Storage Capacity Estimation,
CSLF-T-2007-04; Melbourne, Australia.
2007. p. 42

[3.6.4] U.S. Department of Energy (DOE).
Carbon Sequestration Atlas of United
States and Canada. Washington: Office
of Fossil Energy; 2007. p. 86

[3.6.5] U.S. Department of Energy (DOE).
Methodology for Development of
Geologic Storage Estimates for Carbon
Dioxide. Washington: Office of Fossil
Energy; 2008. p. 36

[3.6.6] Bachu S, Bonijoly D, Bradshaw J,
Burrus R, Holloway S, Christensen NP,
et al. CO2 storage capacity estimation
methodology and gaps. Internationa
Journal of Greenhouse Gas Control.
2007;**1**(4):430-443

[3.6.7] Koide H, Tazaki Y, Noguchi Y,
Nakayama S, Iijima M, Ito K, et al.
Subterranean containment and longterm
storage of carbon dioxide in
unused aquifers and in depleted natural
gas reservoirs. Energy Conversion and
Management. 1992;**33**(5/8):619-626

[3.6.8] Koide H, Tazaki Y, Noguchi Y,
Iijima M, Ito K, Shindo Y. Underground
storage of carbon dioxide in depleted
natural gas reservoirs and in useless

aquifers. Engineering Geology.
1993;**34**(3/4):175-179

[3.6.9] Van der Meer L. Investigations
regarding the storage of carbon
dioxide in aquifers in the Netherlands.
Energy Conversion and Management.
1992;**33**(5/8):611-618

[3.6.10] Ormerod WG, Webster IC,
Ausdus H, Reimer PWF. An overview
of large scale CO2 disposal options.
Energy Conversion and Management.
1993;**34**(9/1):833-840

[3.6.11] Hendriks CA, Blok K. Underground
storage of carbon dioxide. Energy
Conversion and Management.
1993;**34**:949-957

[3.6.13] Novak K. Modeliranje površinskoga
transporta i geološki aspekti skladištenja
ugljikova dioksida u neogenska
pješčenjačka ležišta Sjeverne Hrvatske
na primjeru polja Ivanić (Surface
Transportation Modelling and
Geological Aspects of Carbon-Dioxide
Storage into Northern Croatian Neogene
Sandstone Reservoirs, Case Study
Ivanić Field) [thesis]. University of
Zagreb, Faculty of Mining, Geology and
Petroleum Engineering; 2015

[3.7.1] Directive 2009/31/EC of the European
Parliament and of the Council of 23
April 2009 on the Geological Storage
of Carbon Dioxide and Amending
Council Directive 85/337/EEC, European
Parliament and Council Directives
2000/60/EC, 2001/80/EC, 2004/35/EC,
2006/12/EC, 2008/1/EC and Regulation
(EC) No 1013/2006. OJ L 140

[3.7.2] Gaurina-Međimurec N, Pašić B.
Design and mechanical integrity of CO2
injection wells. The Mining-Geology-
Petroleum Engineering Bulletin.
2011;**23**:1-8

[3.7.3] Gasda S, Bachu S, Celia MA. The potential for CO2 leakage from storage sites in geological media: Analysis of well distribution in mature sedimentary basin. Environmental Geology. 2004;**46**(6-7):707-720

[3.7.4] Gaurina-Međimurec N. The influence of CO2 on well cement. The Mining-Geology-Petroleum Engineering Bulletin. 2010;**22**:19-25

[3.8.1] Carbon Capture and Sequestration Technologies at Massachusetts Institute of Technology (MIT) [Internet]. Available from: https://sequestration.mit.edu [Accessed: 2 December 2018]

[3.8.2] Global CCS Institute [Internet]. Available from: https://www.globalccsinstitute.com [Accessed: 2 December 2018]

[3.8.3] USA National Energy Technology Laboratory (NETL) [Internet]. Available from: https://www.netl.doe.gov [Accessed: 2 December 2018].

[3.8.4] Zero Emissions Platform Database [Internet]. Available from: http://www.zeroemissionsplatform.eu/ [Accessed: 2 December 2018]

[3.8.5] CO2 Stored Database [Internet]. Available from: http://www.co2stored.co.uk/home/index [Accessed: 2 December 2018]

[3.8.5] Gaurina-Međimurec N, Novak Mavar K, Majić M. Carbon capture and storage (CCS): Technology, projects and monitoring review. The Mining-Geological-Petroleum Engineering Bulletin. 2018;**33**:1-15. DOI: 10.17794/rgn.2018.2.1

[3.9.1] Intergovernmental Panel on Climate
Change (IPCC). Special Report on
Carbon Dioxide Capture and Storage.
Cambridge, UK: Cambridge University
Press; 2005. p. 431

[3.9.2] International Energy Agency
(IEA). Interaction of CO2 Storage with
Subsurface Resources. Report: 2013-08.
UK: IEA Environmental Projects Ltd.
(IEAGHG); 2013. p. 115

[3.10.1] Kneafsey, T.J., Pruess, K., 2010. Laboratory flow experiments for visualizing carbon dioxide-induced, density-driven brine convection. Transp. Porous Media 82, 123.

[4.1.0] R.D. Neidinger, Introduction to automatic differentiation and MATLAB object-oriented programming, SIAM Rev. 52 (3) (2010) 545–563, http://dx.doi.org/10.1137/080743627.
[4.1.1] P. Bastian, M. Blatt, A. Dedner, C. Engwer, R. Kl¨ofkorn, M. Ohlberger, O. Sander, A generic grid interface for parallel and adaptive scientific computing. Part I: Abstract framework, Computing 82 (2–3) (2008) 103–119. doi:10.1007/s00607-008-0003-x

[4.1.2] B. Flemisch, M. Darcis, K. Erbertseder, B. Faigle, A. Lauser, K. Mosthaf, S. M¨uthing, P. Nuske, A. Tatomir, M. Wolff, R. Helmig, DuMux: DUNE for multi-{phase,component,scale,physics,...} flow and transport in porous media, Advances in Water Resources 34 (9) (2011) 1102–1112. doi:10. 1016/j.advwatres.2011.03.007.

[4.1.3] E. G. Boman, U. V. Catalyurek, C. Chevalier, K. D. Devine, The Zoltan and Isorropia parallel toolkits for combinatorial scientific computing: Partitioning, ordering, and coloring, Scientific Programming 20 (2) (2012) 129– 150. doi:10.3233/SPR-2012-0342.

[4.1.4] K.-A. Lie, S. Krogstad, I. S. Ligaarden, J. R. Natvig, H. M. Nilsen, B. Skaflestad, Open-source matlab implementation of consistent discretisations on complex grids, Computational Geosciences 16 (2) (2011) 297–322. doi:10.1007/s10596-011-9244-4.

[4.1.5] S. Krogstad, K.-A. Lie, O. Møyner, H. M. Nilsen, X. Raynaud, B. Skaflestad, MRST-AD - an open-source framework for rapid prototyping and evaluation of reservoir simulation problems, in: Reservoir simulation Symposium, Houston, Texas, USA, 23-25 February, 2015. doi: 10.2118/173317-MS.

[4.1.6] K.-A. Lie, An Introduction to Reservoir Simulation Using MATLAB/GNU Octave: User Guide for the MATLAB Reservoir Simulation Toolbox (MRST), Cambridge University Press, 2019. doi:10.1017/ 9781108591416.

[4.1.A]according to Span and Wagner (1996).

[4.1.A2] Duan & Sun, Chemical Geology 193 (2003) 257-271

[4.4.1]Experimental Study on the Density-Driven Carbon Dioxide
Convective Diffusion in Formation Water at Reservoir Conditions
Yongqiang Tang,† Zihao Li,‡ Rui Wang,† Maolei Cui,† Xin Wang,† Zengmin Lun,† and Yu Lu*,§
†Petroleum Exploration and Production Research Institute, Sinopec, Beijing 100083, China
‡Department of Mining and Minerals Engineering, Virginia Tech, Blacksburg, Virginia 24061, United States
§School of Business, Beijing Technology and Business University, Beijing 100048, China

[4.4.2] Slim, C. A.; Bandi, M. M.; Miller, C. J.; et al. Dissolution-driven
convection in a Hele-Shaw cell. Phys. Fluids 2013, 25, 024101.

[4.4.3] Wang, S.; Hou, J.; Liu, B.; et al. The Pressure-decay Method for Nature Convection Accelerated Diffusion of CO2 in Oil and Water under Elevated Pressures. Energy Sources, Part A 2013, 35, 538−545.

[4.4.4] Etminan, S. R.; Maini, B. B.; Chen, Z.; et al. Constant-pressure technique for gas diffusivity and solubility measurements in heavy oil and bitumen. Energy Fuels 2010, 24, 533−549.